Optimization and Reduced-Order Modeling of Geological Carbon Storage Operations

Louis J. Durlofsky

Department of Energy Resources Engineering
Stanford University

Key Collaborators on Work Presented

- **David Cameron** (optimization of carbon storage operations)
- **Z. Larry Jin** (ROM for CO_2 injection, building on work by **Jincong He**)
- **Sumeet Trehan** (ROM for oil/water)

Carbon Capture and Storage

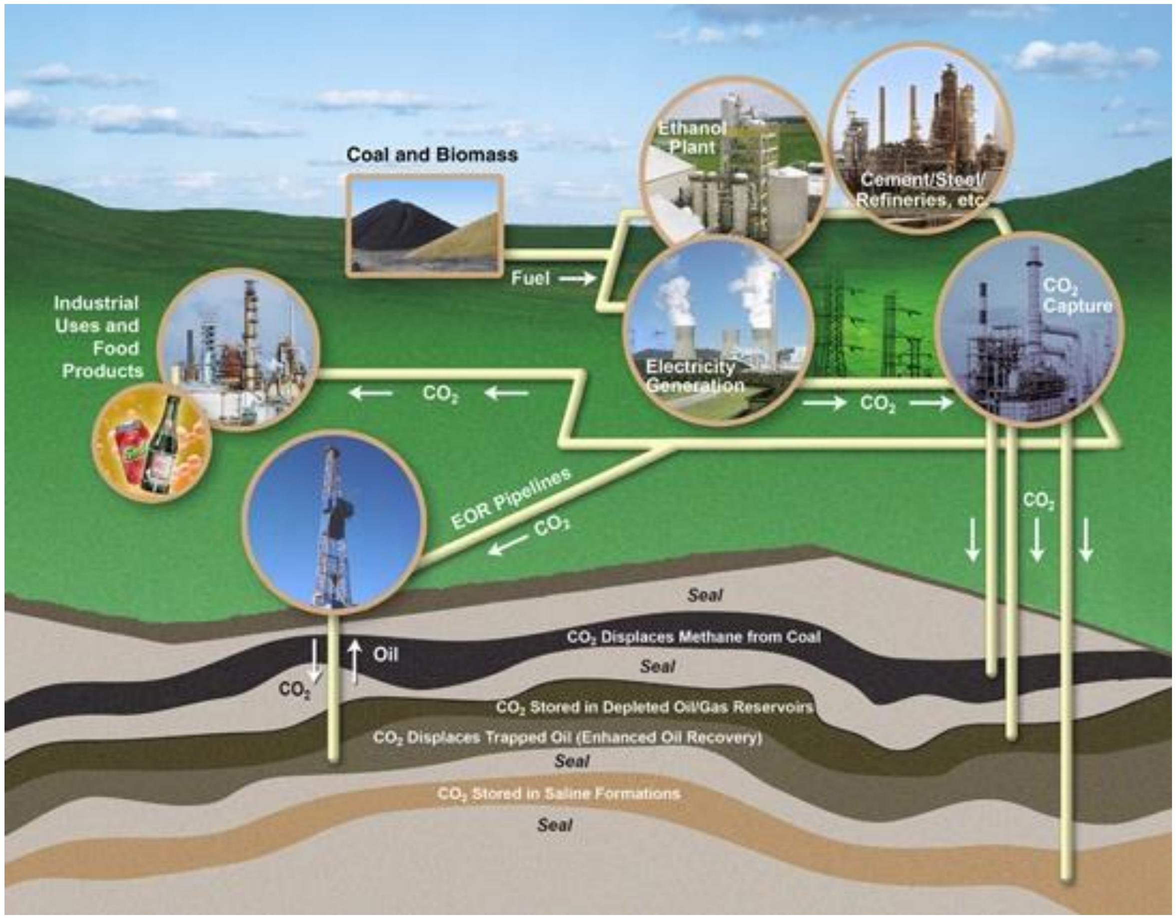

https://energy.gov/fe/science-innovation/carbon-capture-and-storage-research/overview-carbon-storage-research

Capture / compress ⟶ Transport ⟶ Inject ⟶ Monitor / remediate

CO_2 Trapping Mechanisms

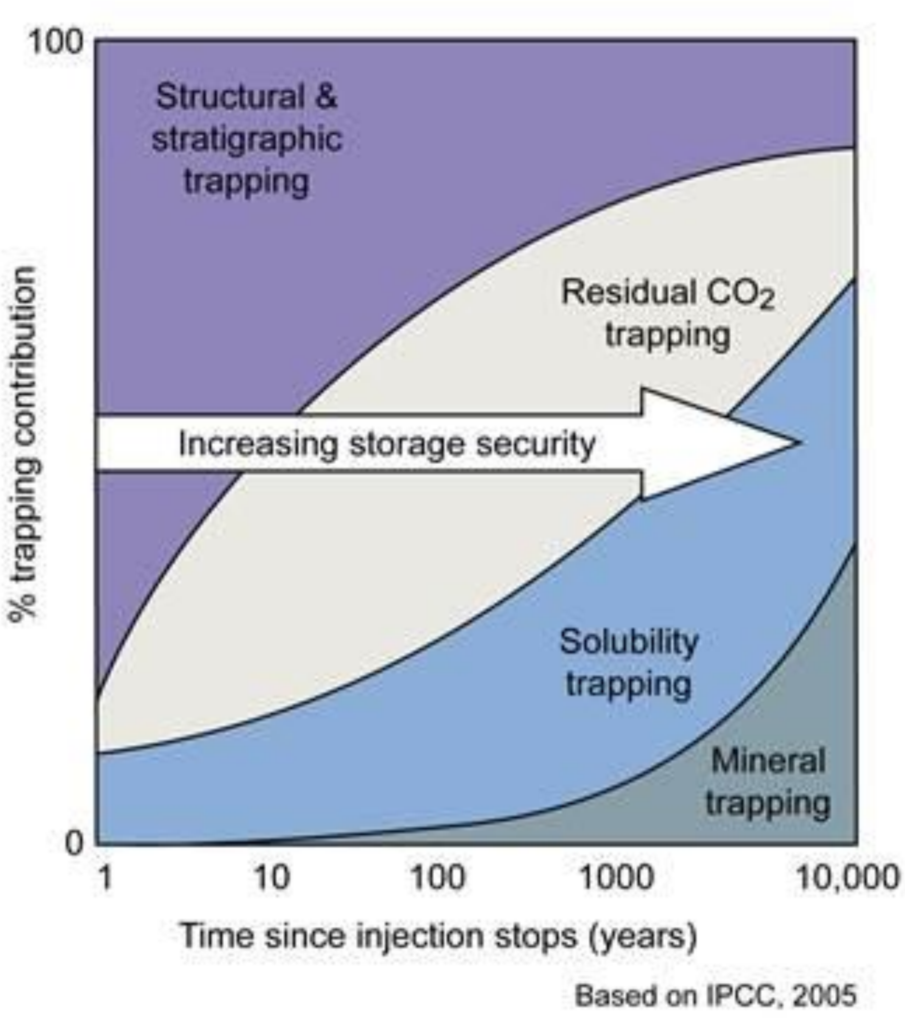

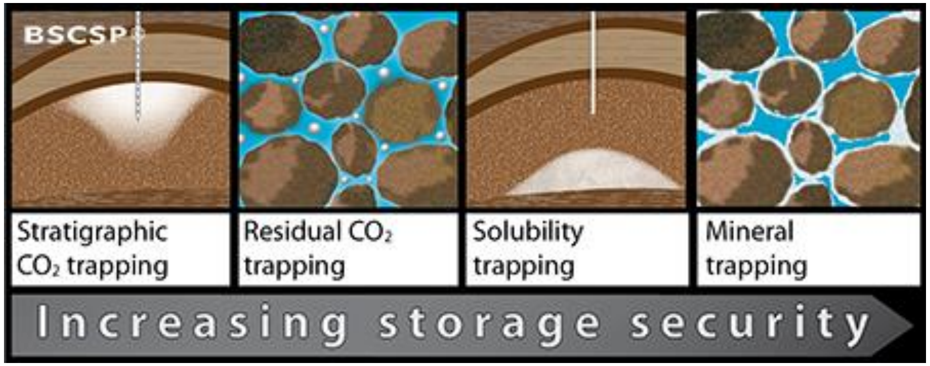

http://www.bigskyco2.org/node/127

https://data.geus.dk/nordiccs/terminology.xhtml

Optimization Problem Statement

- Minimize measure of aggregate mobility of CO_2 in target region (e.g., just below cap rock) over *T* years:

$$\min_{\mathbf{y},\mathbf{u}} J(\mathbf{y},\mathbf{u}) = \frac{1}{T} \int_{t=0}^{T} \sum_{i \in \text{top layer}} \left(\frac{\rho_g k_{rg}}{\mu_g} \right)_i dt$$

$\mathbf{y}$: well placement variables, $\mathbf{u}$: injection rate variables

- With uncertainty, $\min E[J(\mathbf{y},\mathbf{u})] \approx (1/N_k) \sum_1^{N_k} J_k(\mathbf{y},\mathbf{u},\mathbf{m}_k)$
- Could define *J* in terms of pressure buildup, well costs, …
- Related work: Shamshiri & Jafarpour (2012), Petvipusit et al. (2014), Babaei et al. (2015, 2016)

Basic Pattern Search

- Local search
- Naturally parallelizable
- Convergence theory based on stencil reduction
- Mesh adaptive direct search (MADS) uses oriented stencil

Optimization in $\mathbb{R}^2$

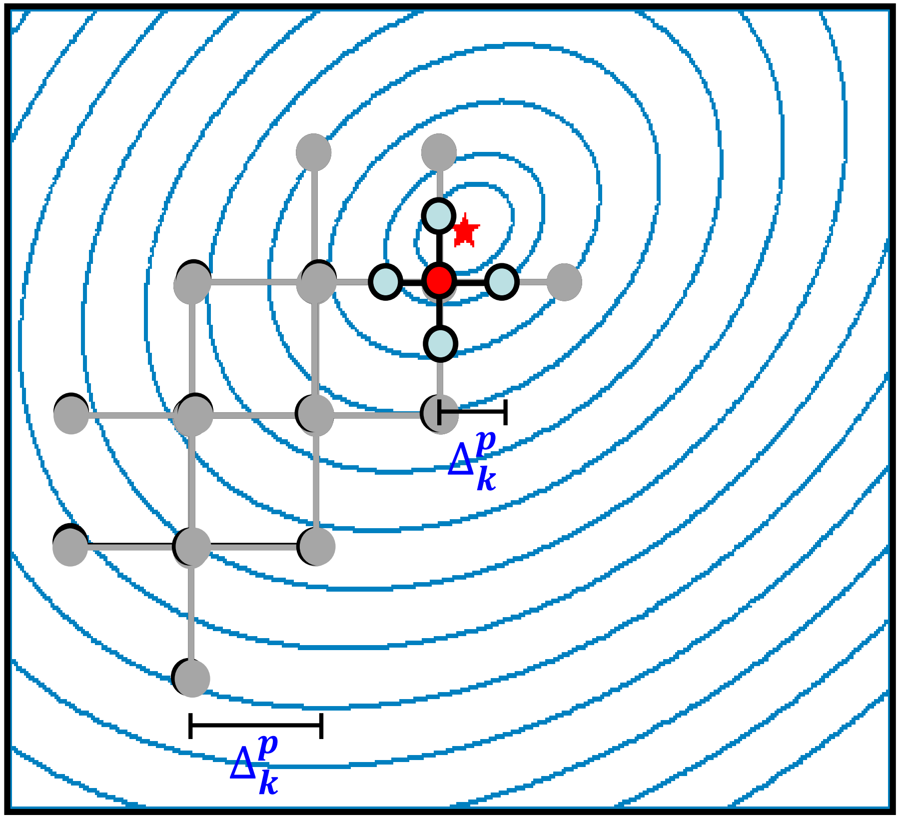

(Kolda et al., 2003;
slide from Obi Isebor)

Particle Swarm Optimization (PSO)

(Eberhart and Kennedy, 1995)

- Global stochastic search
- Solutions are particles in a swarm
- Solution update given by:

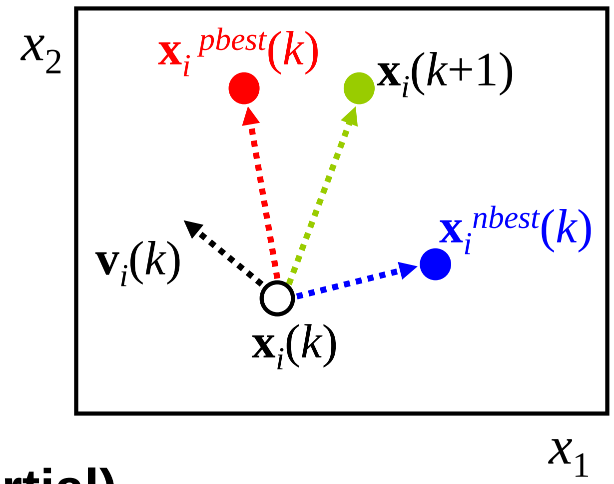

$$\mathbf{x}_i(k+1) = \mathbf{x}_i(k) + \mathbf{v}_i(k+1)\cdot\Delta t$$

$$\mathbf{v}_i(k+1) = \omega\cdot\mathbf{v}_i(k) \quad \textbf{(inertial)}$$

$$+\, c_1\cdot D_1(k)\cdot(\mathbf{x}_i^{pbest}(k) - \mathbf{x}_i(k)) \quad \textbf{(cognitive)}$$

$$+\, c_2\cdot D_2(k)\cdot(\mathbf{x}_i^{nbest}(k) - \mathbf{x}_i(k)) \quad \textbf{(social)}$$

PSO parameters: $\omega, c_1, c_2; \quad D_1(k), D_2(k) \sim U(0,1)$

Can globally explore solution space; no guarantees of convergence

PSO-MADS Hybrid Algorithm*

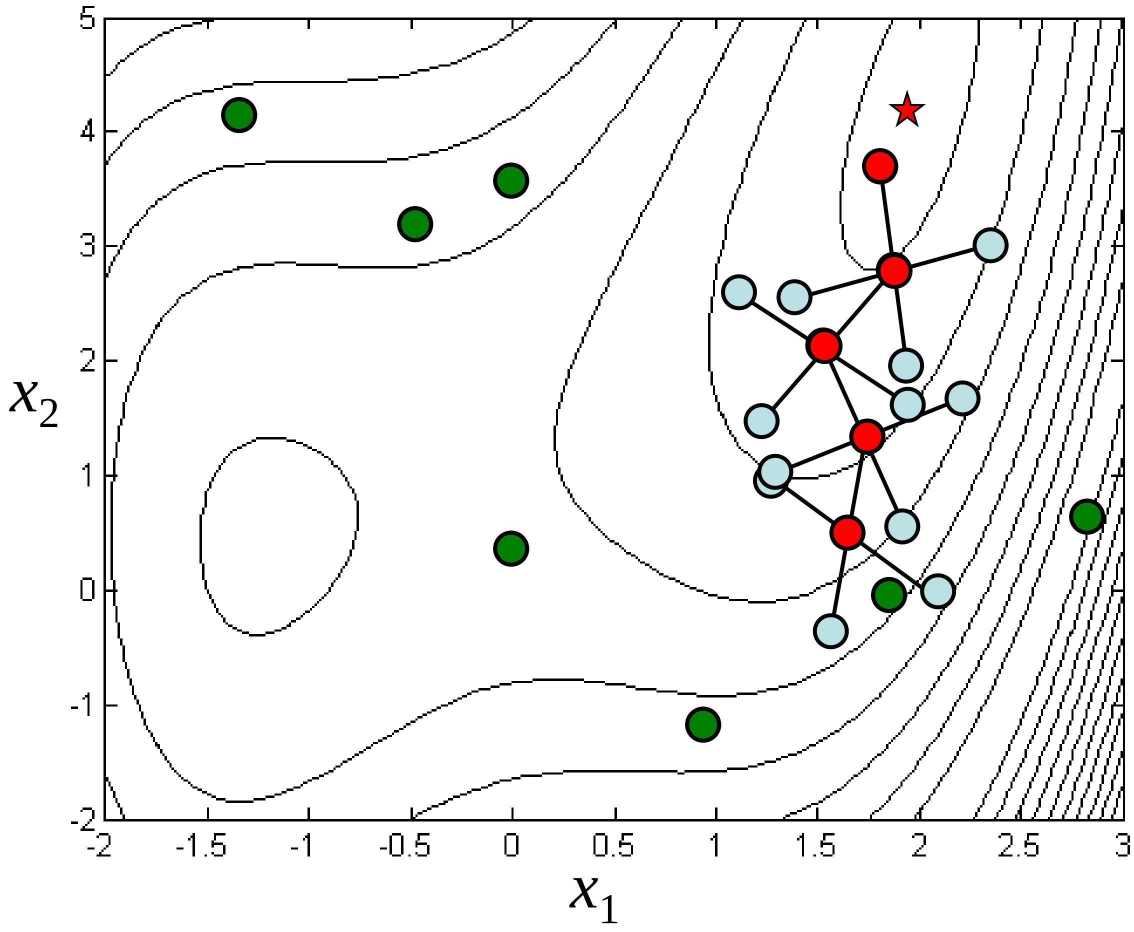

*Isebor, Echeverría Ciaurri, Durlofsky (2014a,b)

Aquifer Simulation Model

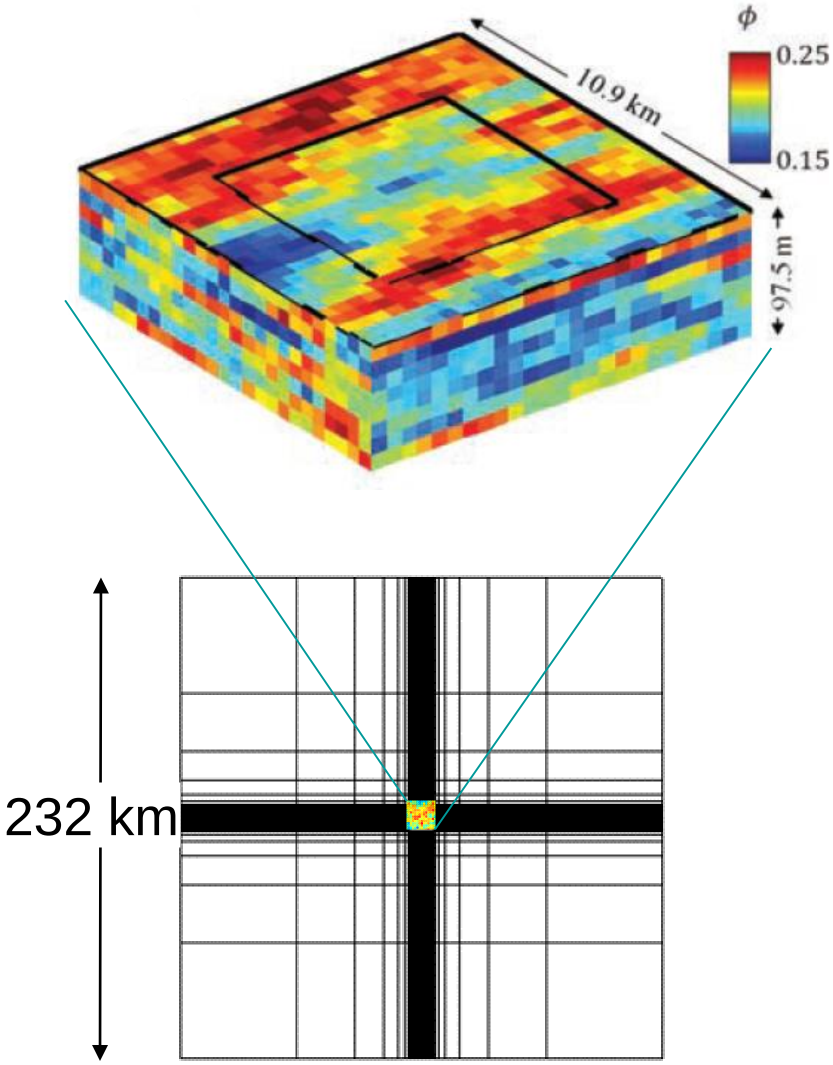

- Grid: 39x39x8
- Large boundary volume to provide pressure support
- Relative permeability hysteresis included; no mineralization or $p_c(\mathbf{x})$

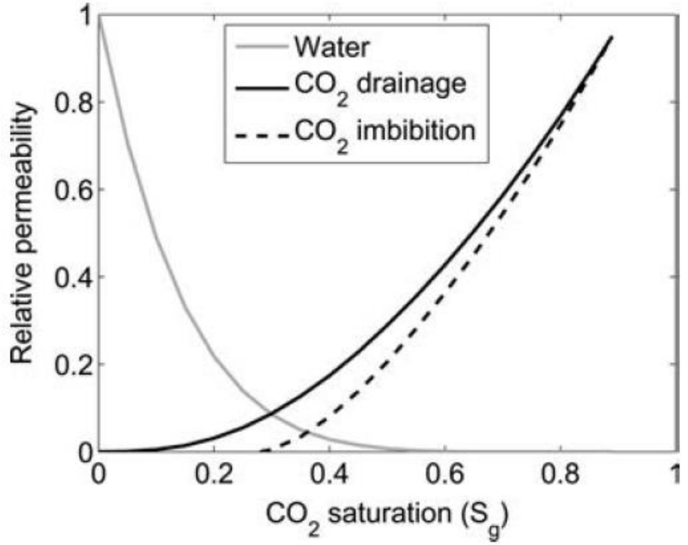

Simulation & Optimization Variables

- (*i, j*) locations of 4 horizontal injection wells (prescribed to be in the bottom layer)
- Rates in each well in 6 control periods (inject 5×10^6 tonnes CO_2 per year for 30 years)
- Corresponds to 2.5% of storage aquifer PV
- N_v = 30 optimization variables (no brine cycling), ~22–30 PSO particles

Minimize CO_2 Mobility (PSO)

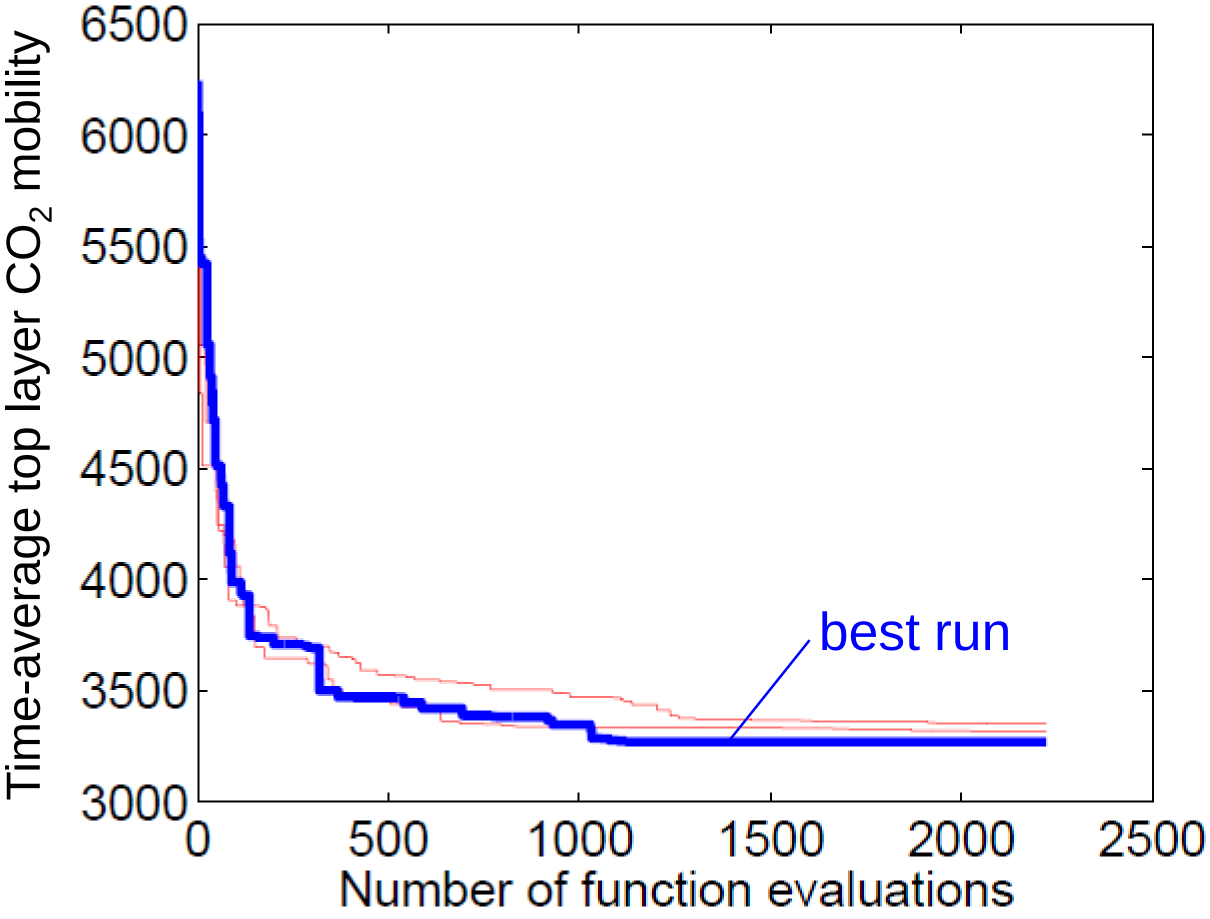

Well Locations and CO_2 Mobility

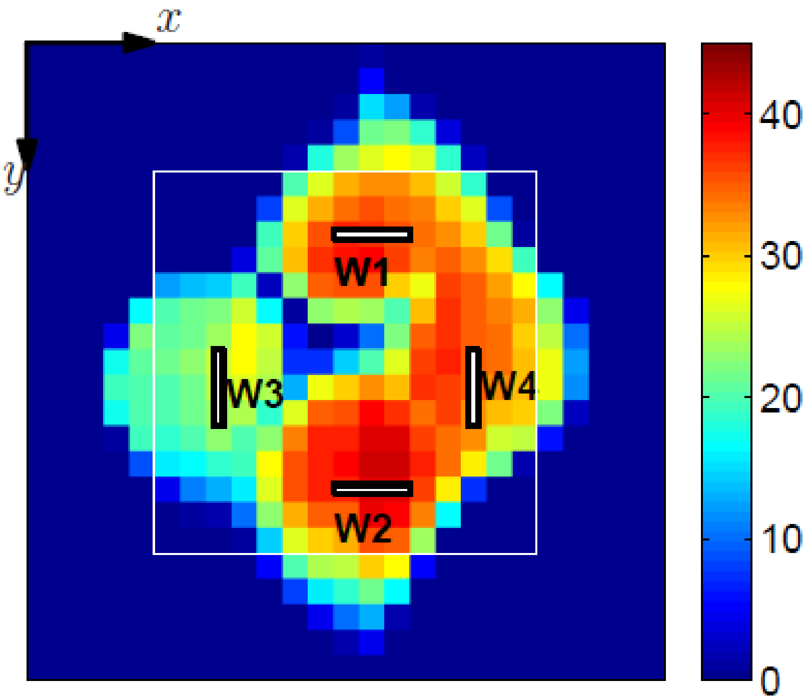

Default

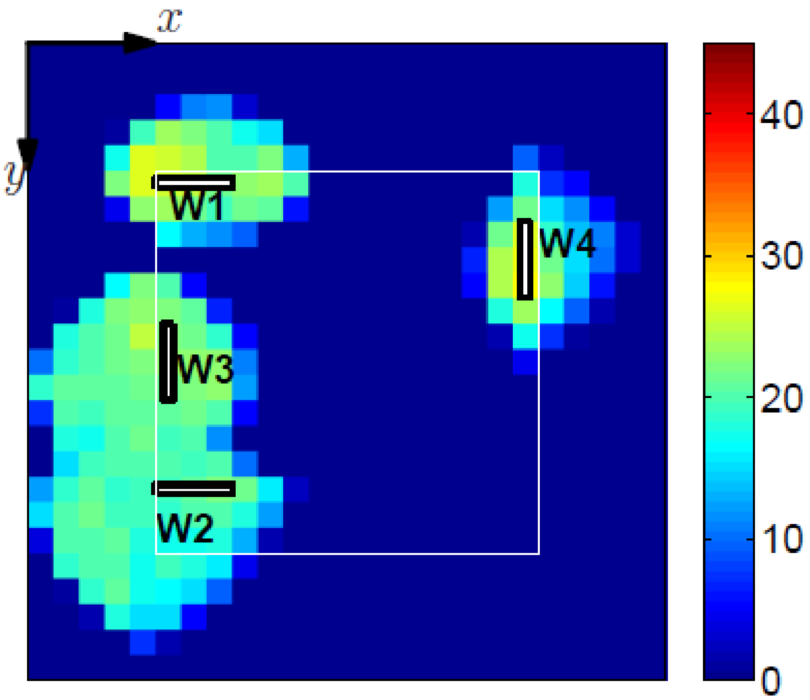

Optimal

Injection wells – bottom layer; CO_2 – top layer

Optimal Injection Rates

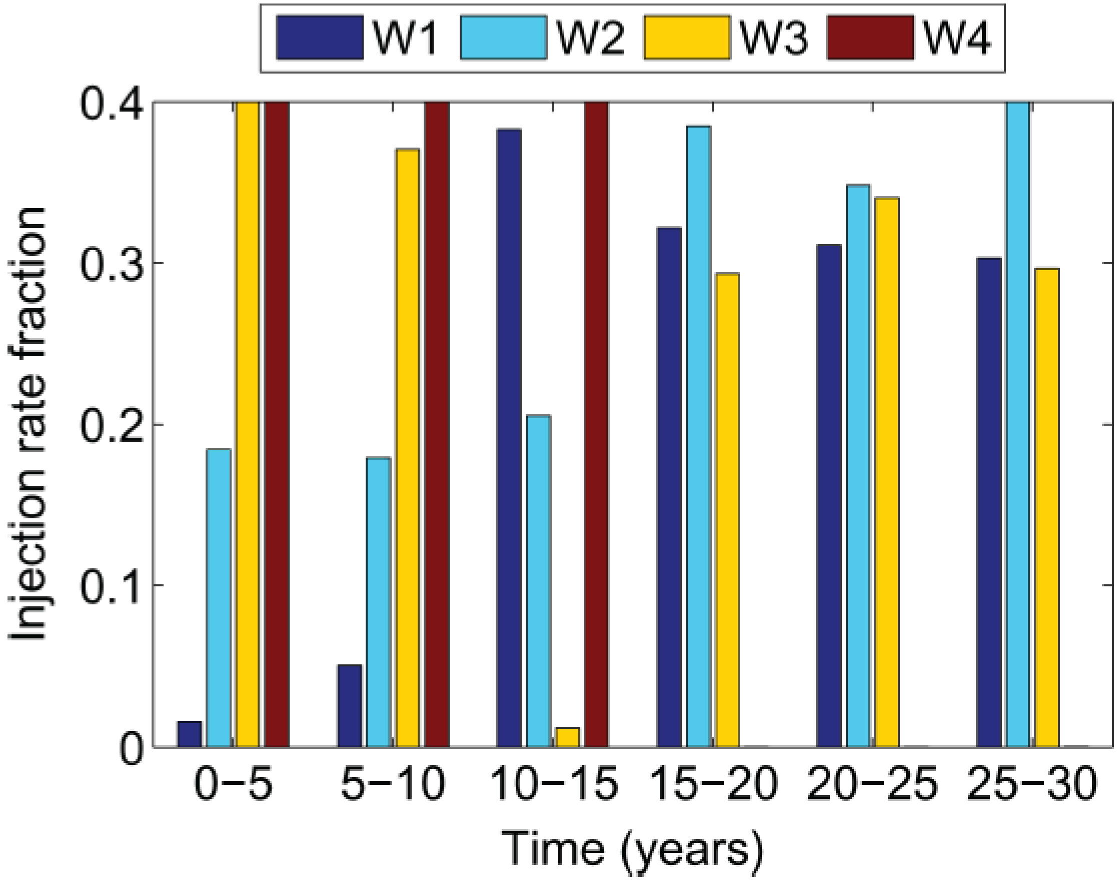

- W4 injects for 15 years; W1 injects more at late times

Mobile CO_2 in Top Layer

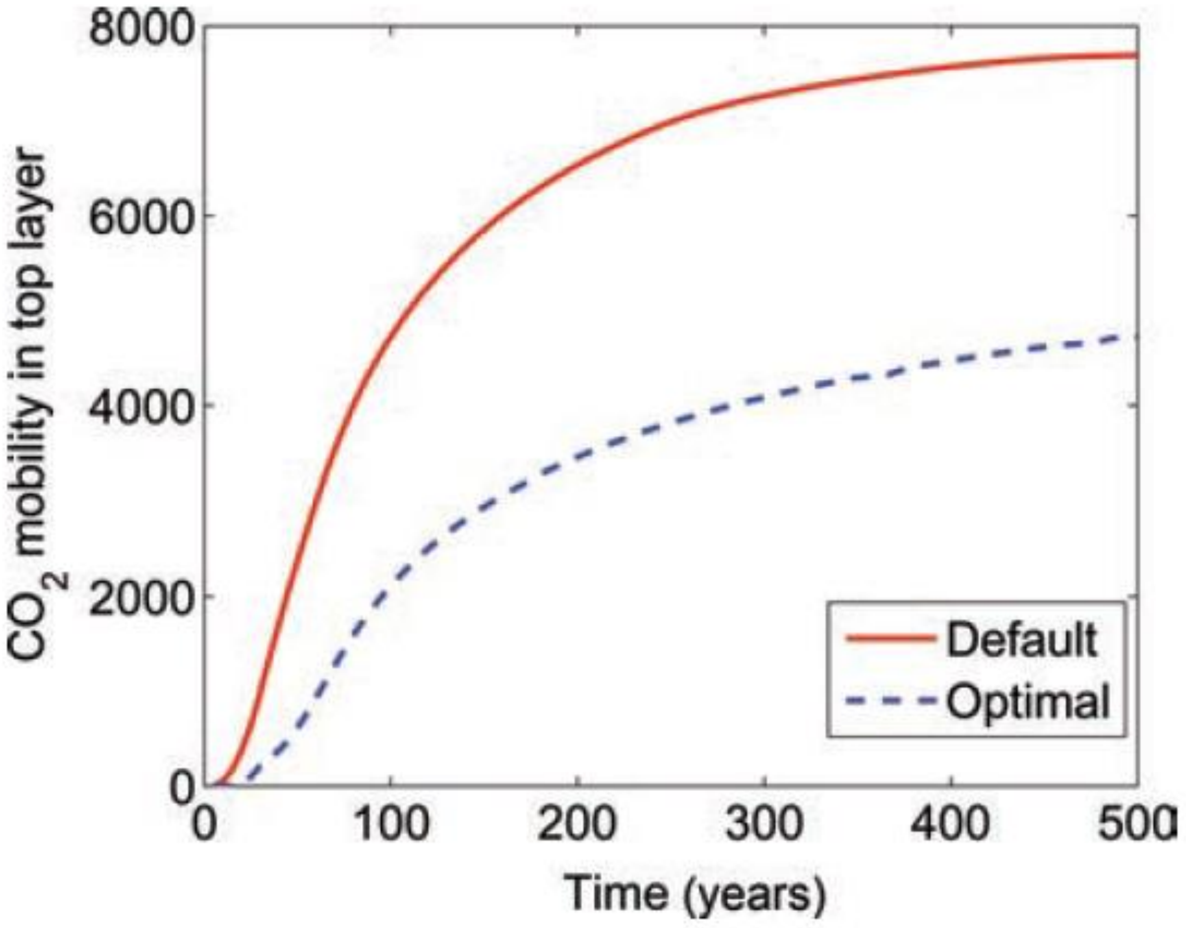

Brine Cycling Strategies in CCS

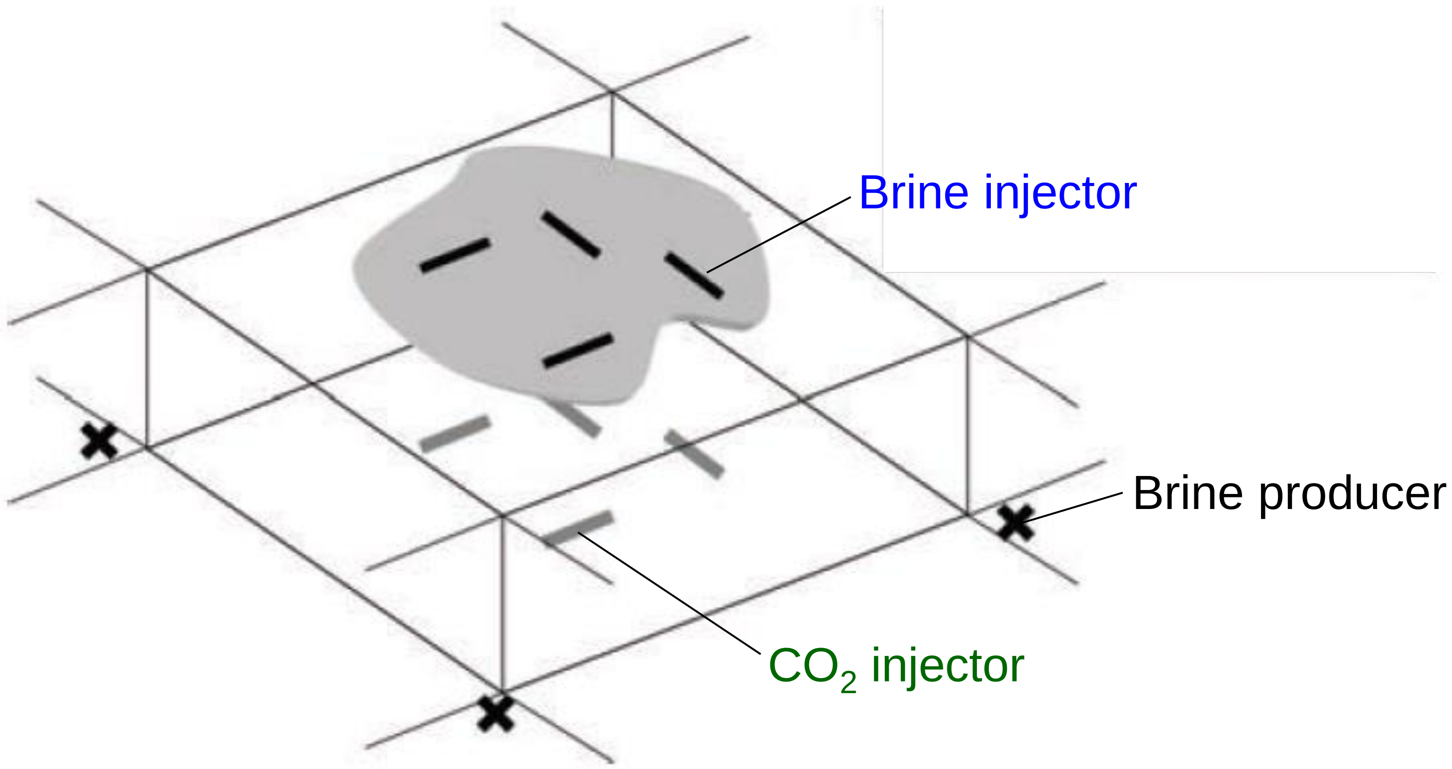

- Related strategies proposed by Leonenko & Keith (2008), Nghiem et al. (2009, 2010), Anchliya (2012)

Brine Cycling Process (illustration)

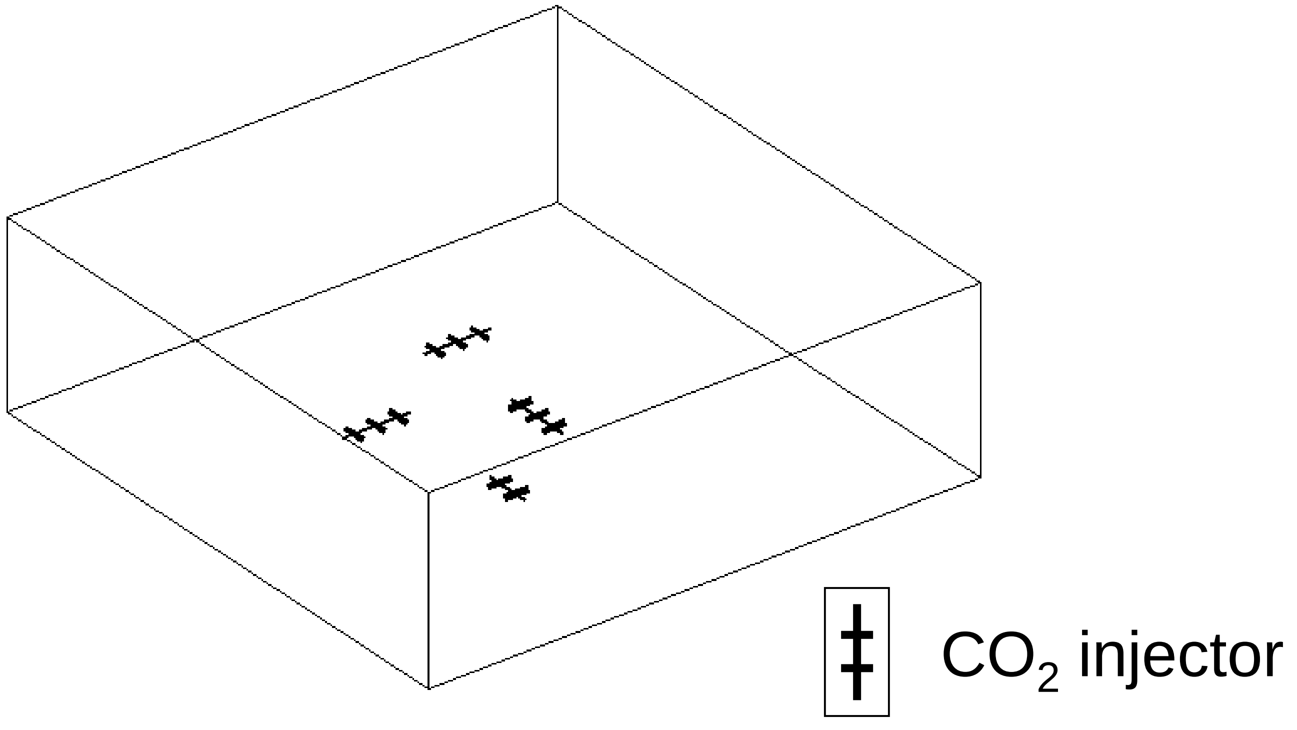

Brine Cycling Process

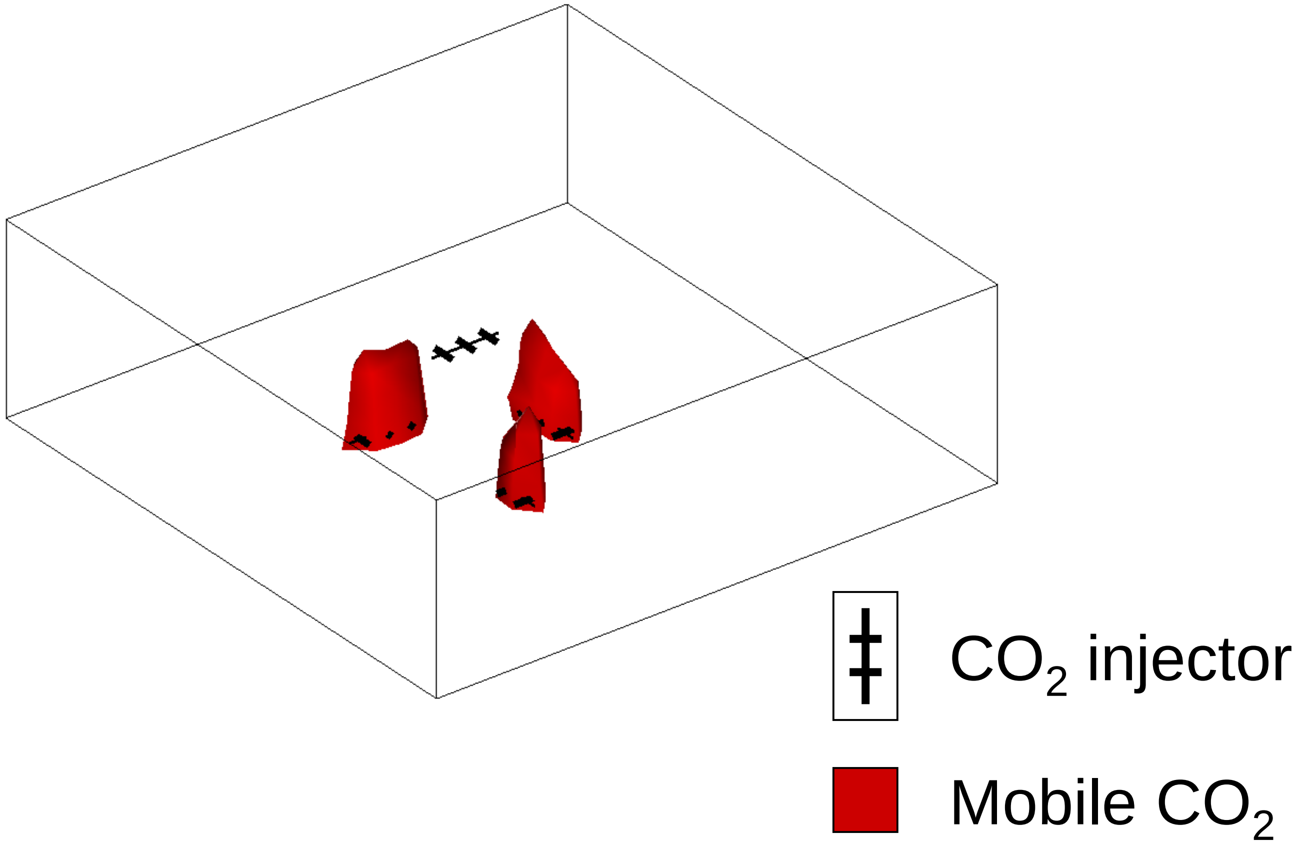

Brine Cycling Process

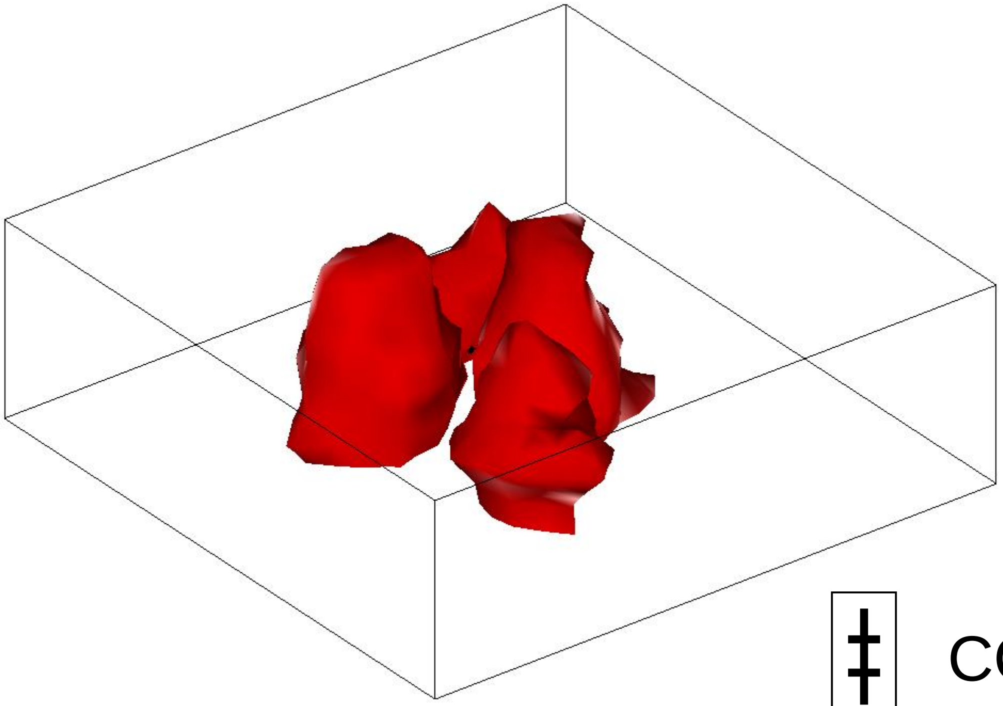

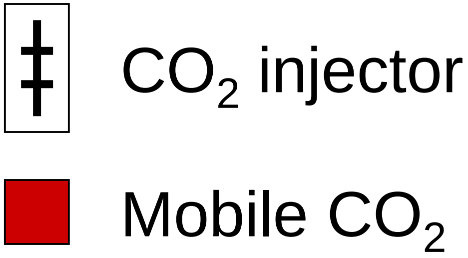

Brine Cycling Process

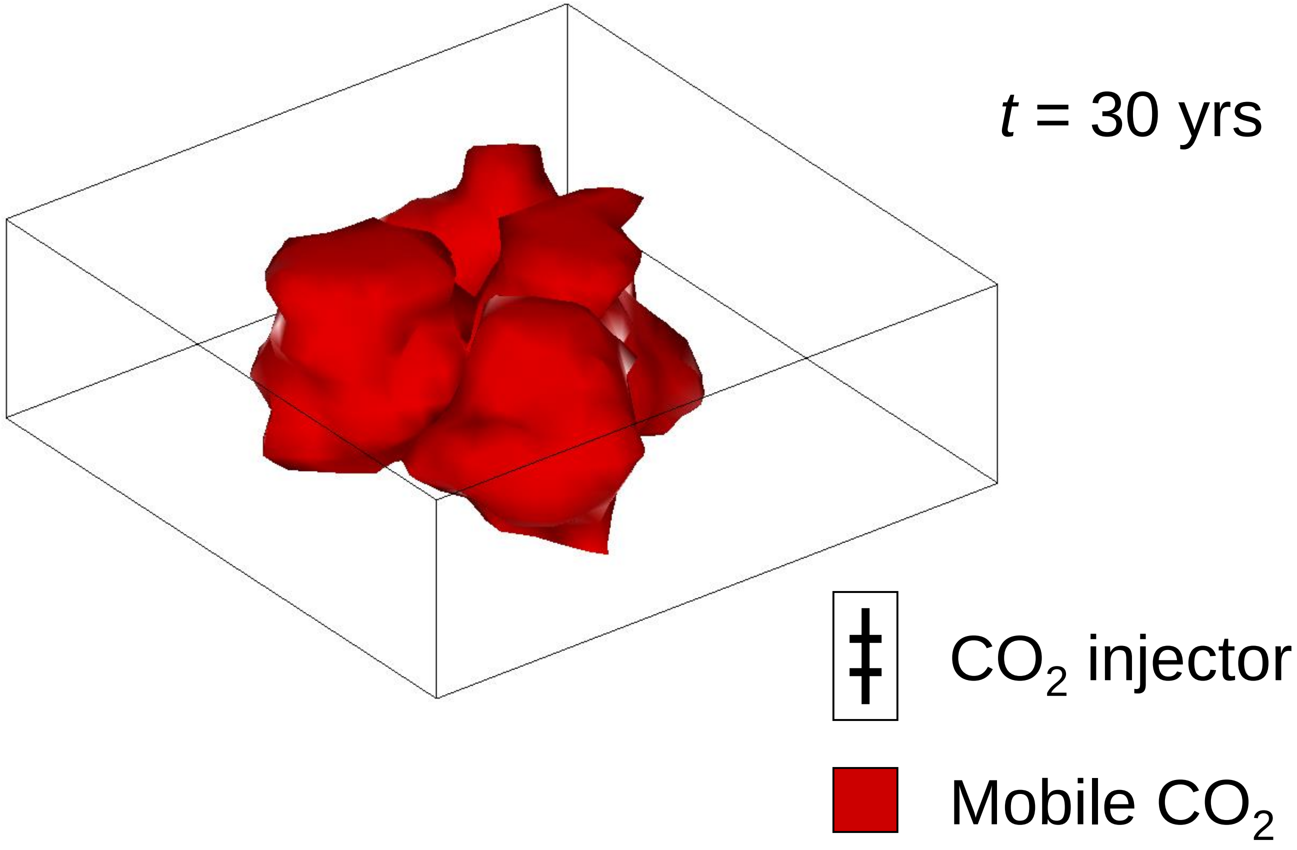

Brine Cycling Process

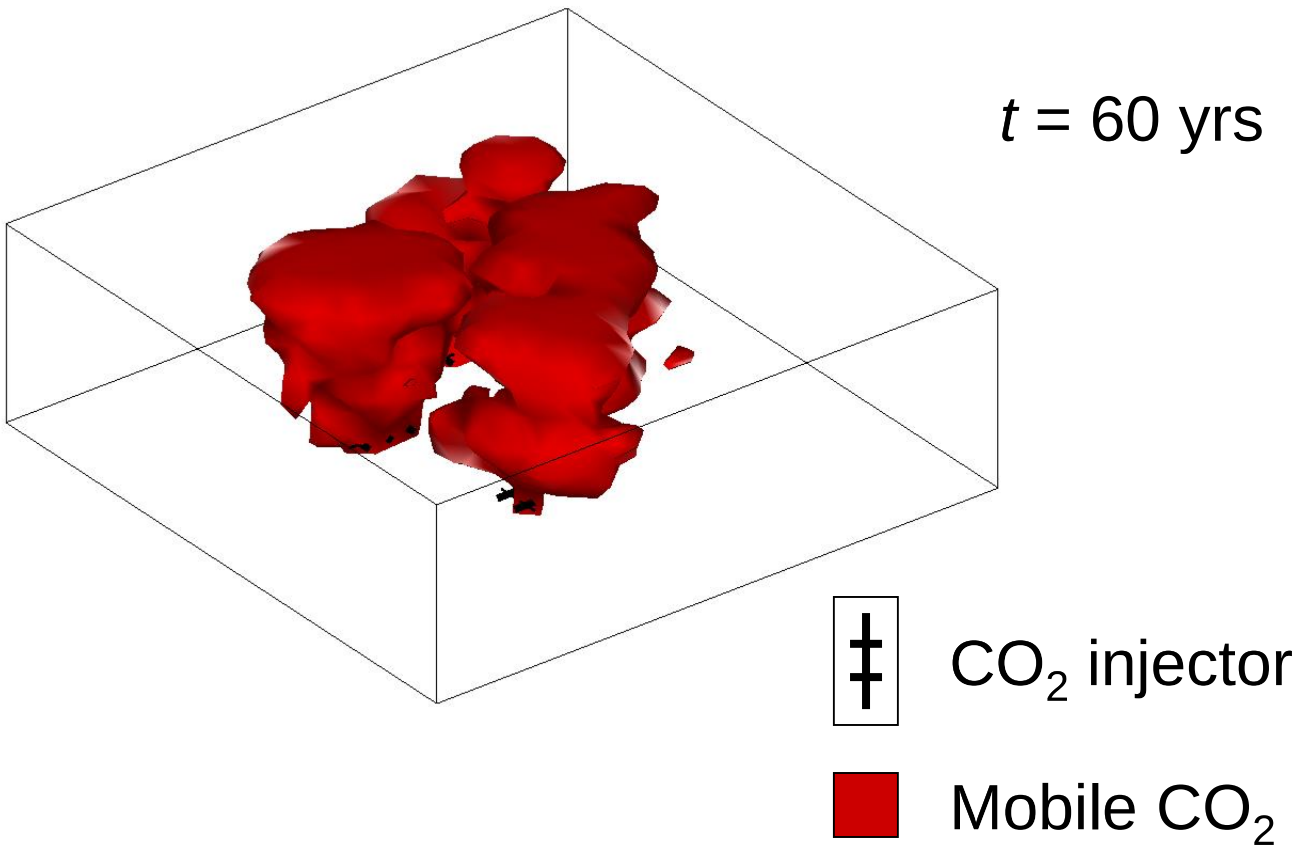

Brine Cycling Process

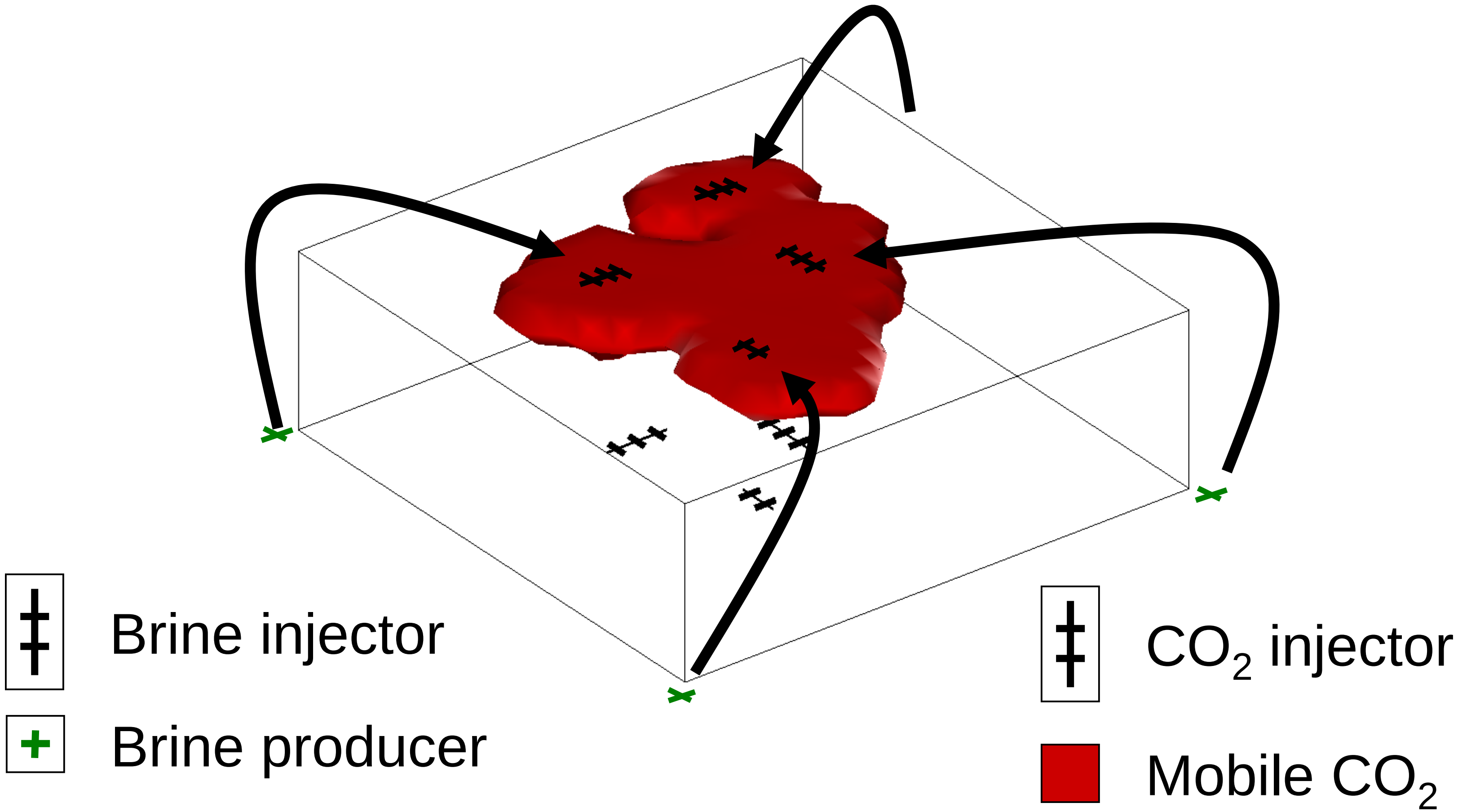

Brine Cycling Process

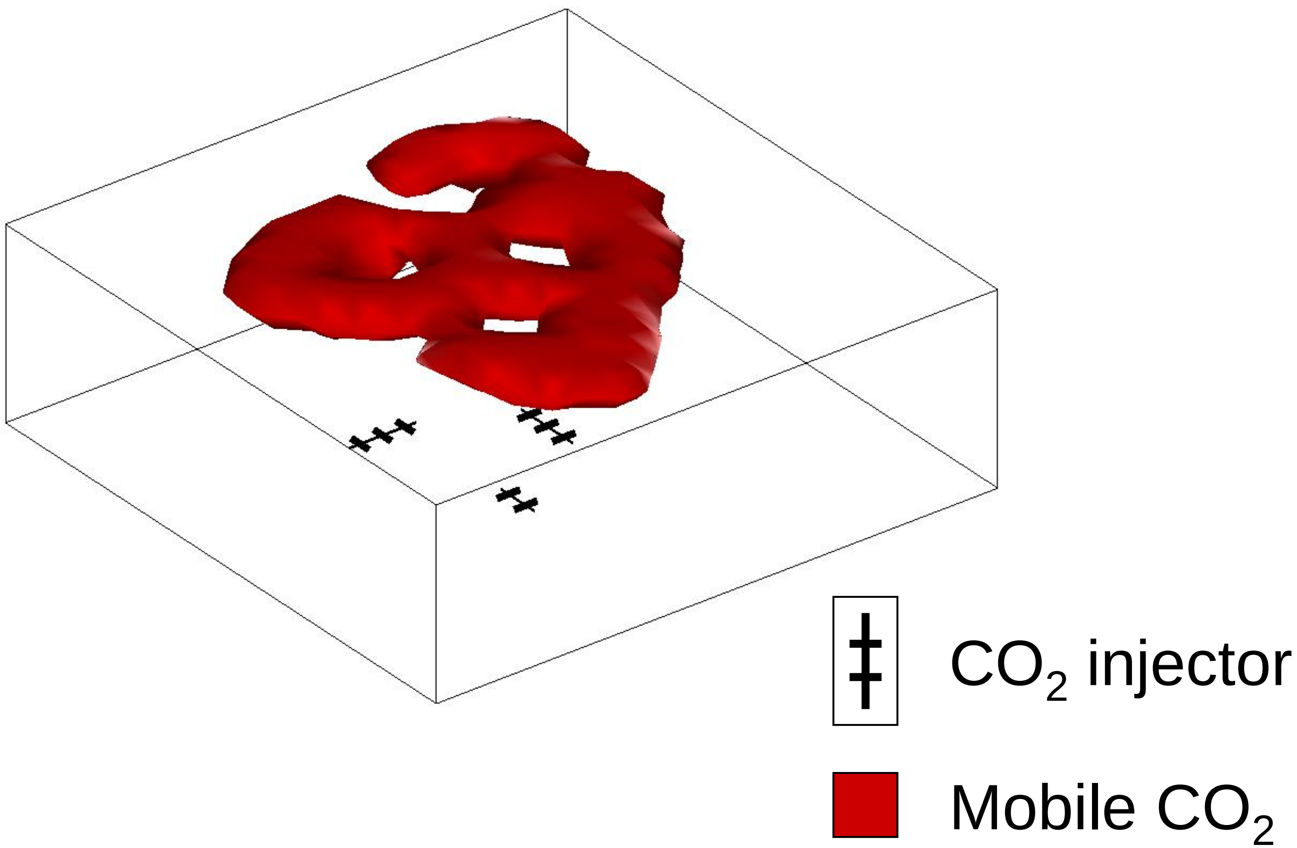

Brine Cycling Process

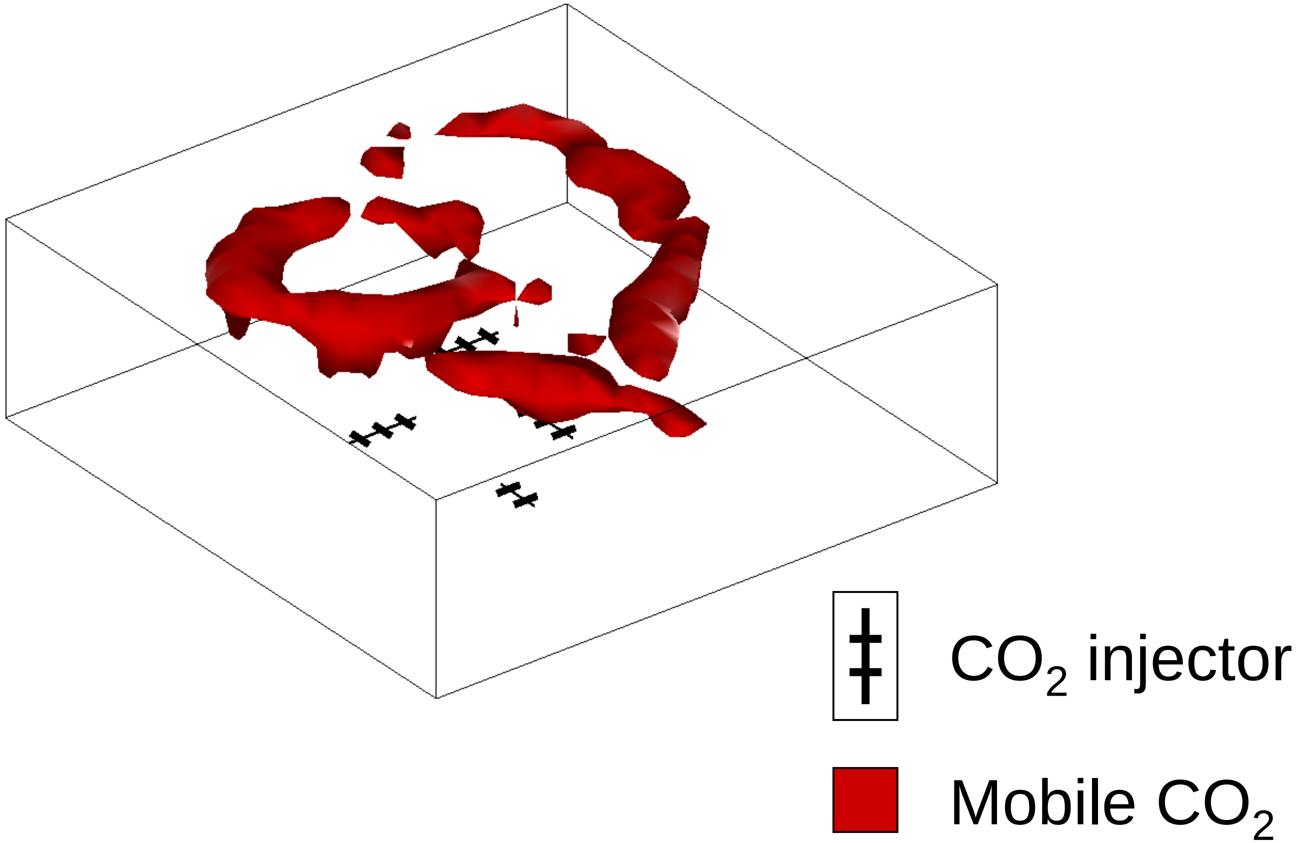

Brine Cycling Process

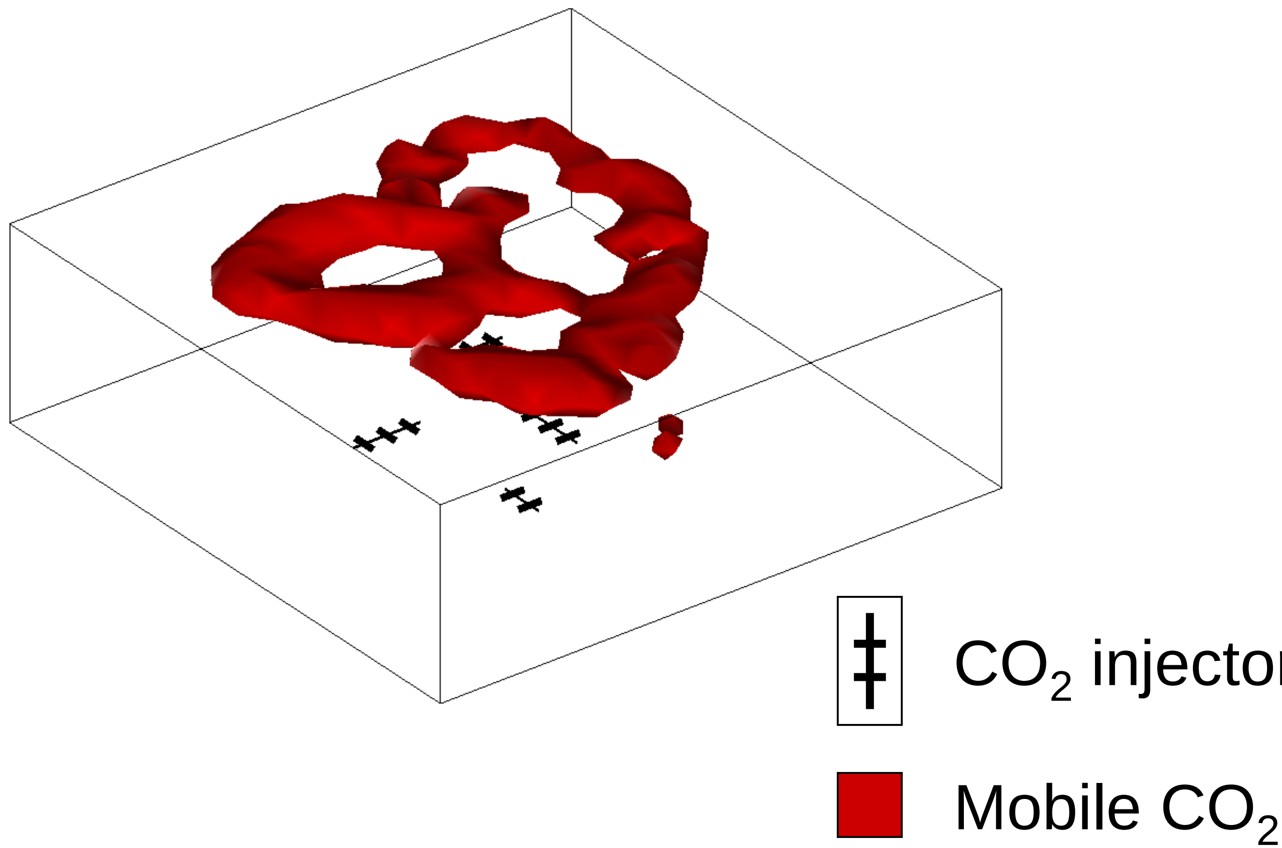

Brine Cycling Optimization

- Minimize measure of aggregate mobility of CO_2 in top or target layer over *T* years:

$$\min_{\mathbf{y},\mathbf{u}_1,\mathbf{u}_2} J(\mathbf{y},\mathbf{u}_1,\mathbf{u}_2) = \frac{1}{T}\int_{t=0}^{T} \sum_{i \in \text{top layer}} \left(\frac{\rho_g k_{rg}}{\mu_g}\right)_i dt$$

y: well placement variables

$\mathbf{u}_1$: injection rate variables

$\mathbf{u}_2$: times and volumes for 3 brine cycling events, subject to specified total brine PV cycled

- Determine total of $N_v = 47$ optimization variables

Brine Cycling Optimization Results

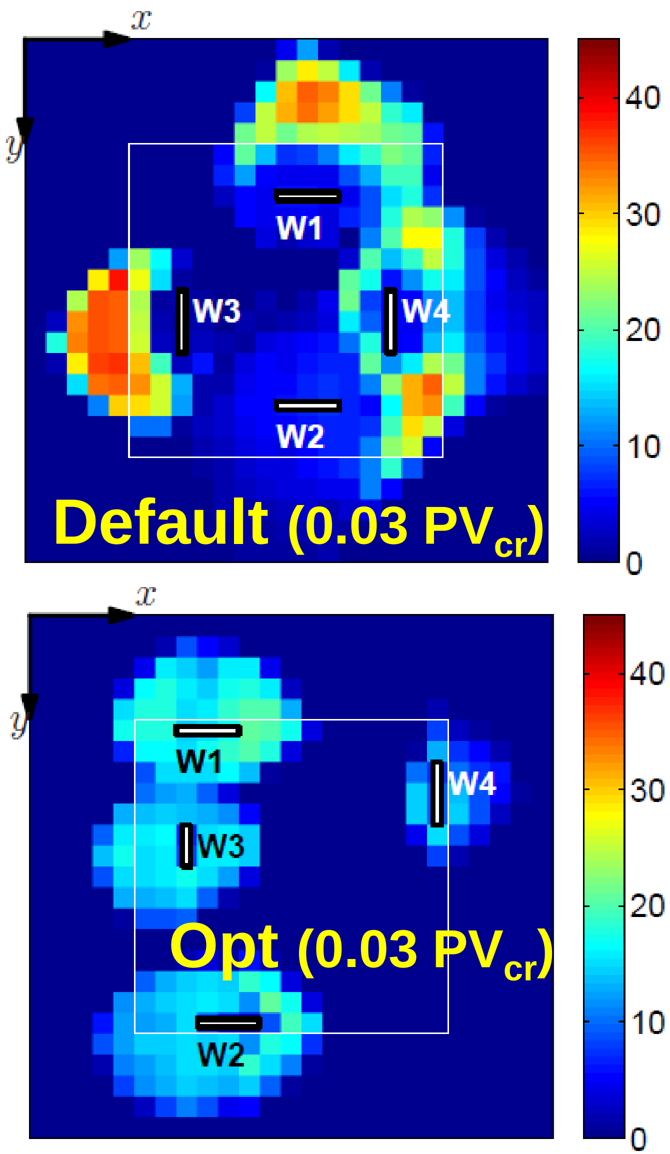

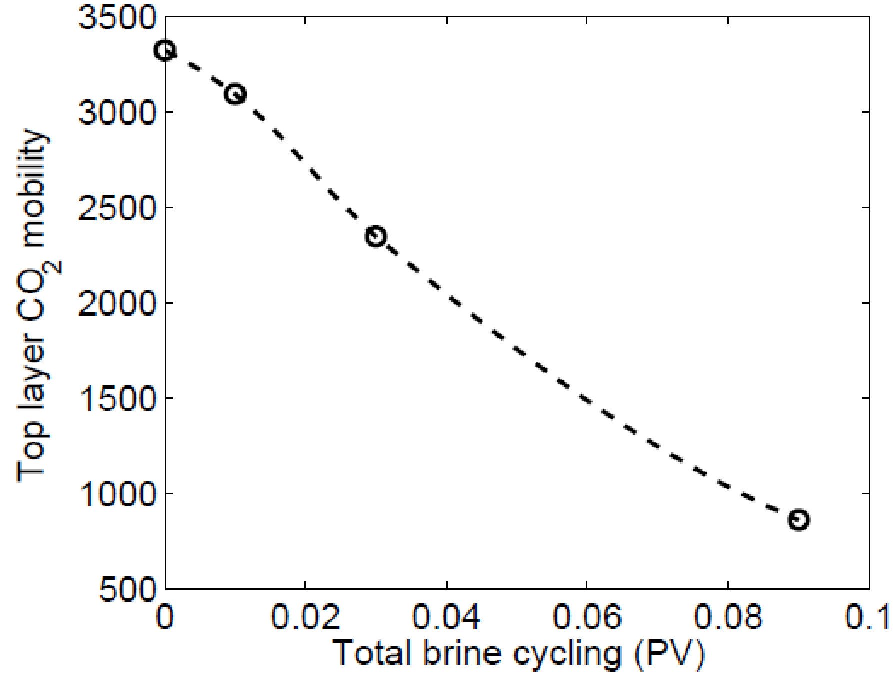

Pore volume as fraction of 15x15x8 core region

(0.03 PV of core region ~0.01 PV of storage aquifer)

Optimization under Geological Uncertainty

- Minimize expected value of time-averaged mobility over N_k prior realizations $\mathbf{m}_k$:

$$E[J(\mathbf{y},\mathbf{u})] \approx \frac{1}{N_k}\sum_{k=1}^{N_k} J_k(\mathbf{y},\mathbf{u},\mathbf{m}_k)$$

$$J_k(\mathbf{y},\mathbf{u},\mathbf{m}_k) = \frac{1}{T}\int_{t=0}^{T} \sum_{i\in t_k} \left(\frac{\rho_g k_{rg}}{\mu_g}\right)_i dt$$

t_k: target layer in model $\mathbf{m}_\mathrm{k}$

- No brine cycling in these examples

Optimization under Geological Uncertainty

- Expected value of time-averaged mobility over $N_k = 10$ prior (Gaussian) realizations

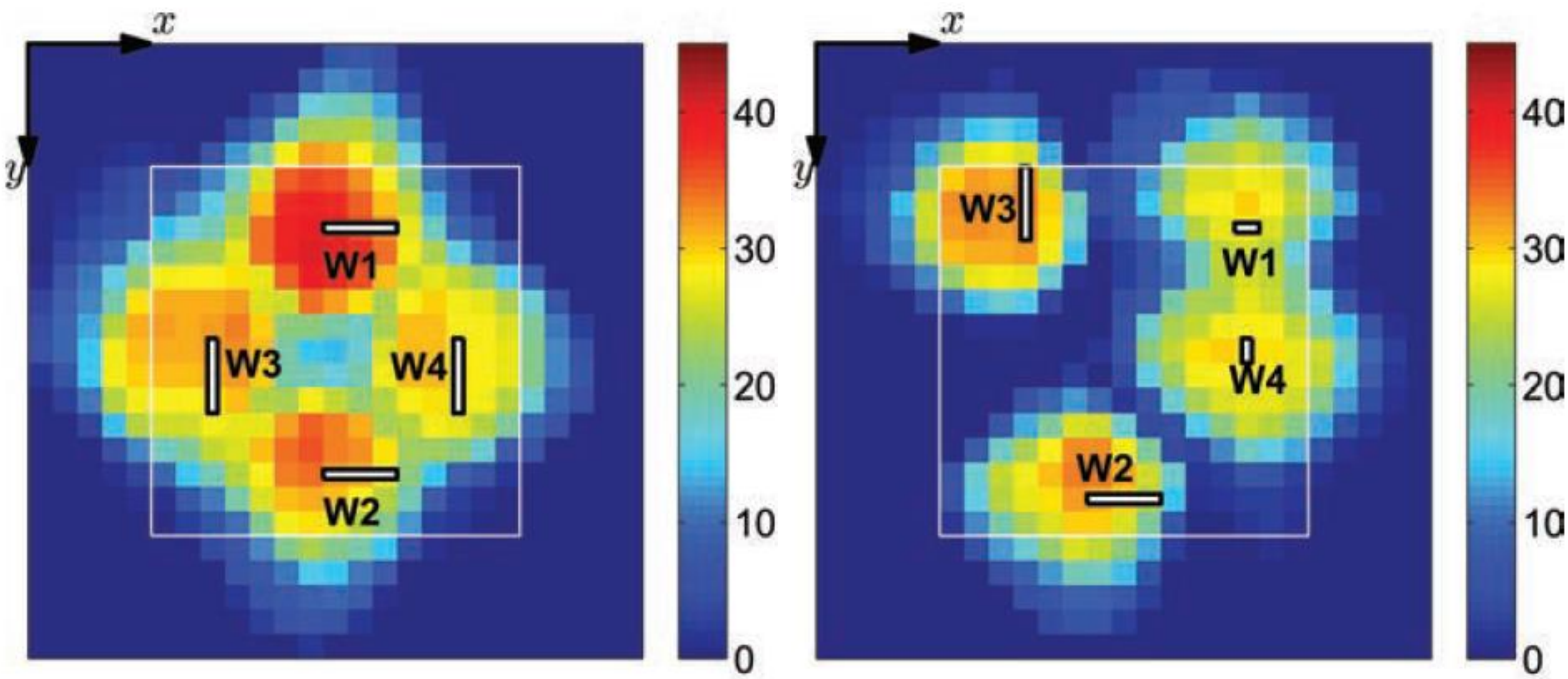

Default (6900)   **Optimized (5300)**

Optimization under Geological Uncertainty (5 new true models)

Model	Default	A priori opt. rates & locs
True 1	6080	4890
True 2	6150	5370
True 3	6380	4660
True 4	9020	7670
True 5	7760	5710
Average	7080	5660

Improvement from a priori optimization ~20%

Optimization under Geological Uncertainty (5 new true models)

Model	Default	A priori opt. rates & locs	Opt. rates with a priori opt. locs
True 1	6080	4890	4670
True 2	6150	5370	4840
True 3	6380	4660	4500
True 4	9020	7670	7280
True 5	7760	5710	4940
Average	7080	5660	5250

Maximum additional improvement from closed-loop, ~7%

Optimization under Geological Uncertainty (5 new true models)

Model	Default	A priori opt. rates & locs	Opt. rates with a priori opt. locs	Deterministic optimization
True 1	6080	4890	4670	3270
True 2	6150	5370	4840	3440
True 3	6380	4660	4500	4500
True 4	9020	7670	7280	6220
True 5	7760	5710	4940	4290
Average	7080	5660	5250	4340

Additional improvement from knowledge of **m**, ~23%

POD-based Reduced-Order Models for Reservoir Simulation (partial list)

- **POD only**: van Doren, Markovinovic, Jansen (2006); Cardoso et al. (2009)
- **POD-DEIM**: Ghasemi, Yang, Gildin, Efendiev, Calo (2015); Yang, Gildin, Efendiev, Calo (2017); Yoon, Alghareeb, Williams (2016)
- **POD-TPWL**: Cardoso & Durlofsky (2010); He et al. (2011,2014,2015); Fragoso, Horowitz, Rodrigues (2015)
- **POD-TPWQ**: Trehan & Durlofsky (2016)
- **ROMs for optimization**: Jansen & Durlofsky (2017)

Proper Orthogonal Decomposition and Trajectory Piecewise Linearization (POD-TPWL)

Basic idea

Use states and derivative matrices generated and saved during training run(s) to represent new solutions

Approach

- Run training simulations ($\mathbf{g}(\mathbf{x},\mathbf{u}) = \mathbf{0}$)
- Record states, Jacobian matrices, etc. ($\mathbf{x}^i, \partial\mathbf{g}^i/\partial\mathbf{x}^i$)
- Represent new solutions ($\mathbf{x}^{n+1}$) as expansions around saved states ($\mathbf{x}^i, \mathbf{x}^{i+1}$)
- Map into low-dim reduced space $\boldsymbol{\xi}$ using **POD ($\mathbf{x} = \boldsymbol{\Phi}\boldsymbol{\xi}$)**

TPWL: Rewienski & White (2003); Vasilyev et al. (2003); Qu & Chapman (2006), …

Gas – Water Flow Equations

- Mass balance equations for *j* = gas, water

$$\phi \frac{\partial s_j}{\partial t} - \nabla \cdot \left(\lambda_j \mathbf{k} \cdot \nabla p\right) + q_j = 0$$

$\boldsymbol{S_j}$ - phase saturation, $\boldsymbol{p}$ - pressure

$\boldsymbol{\lambda_j(S_j)}$ - phase mobility, $\mathbf{k}$ - permeability tensor, $\boldsymbol{q_j}$ - source

- Discretize: $\mathbf{x}$ - states (p, S_w), $\mathbf{u}$ - controls ($\boldsymbol{p}_{\mathbf{well}}$),
  O(10^4 - 10^6) grid blocks (n_b)

$$\mathbf{g}(\mathbf{x}^{n+1}, \mathbf{x}^{n}, \mathbf{u}^{n+1}) = \mathbf{A}(\mathbf{x}^{n+1}, \mathbf{x}^{n}) + \mathbf{F}(\mathbf{x}^{n+1}) + \mathbf{Q}(\mathbf{x}^{n+1}, \mathbf{u}^{n+1}) = \mathbf{0}$$

- Newton's method: $\boldsymbol{J\delta = -\mathbf{g}}\,,\;\; \boldsymbol{J = \partial \mathbf{g} / \partial \mathbf{x}}$

TPWL for Reservoir Flow Equations

Discretized flow equations:

$$\mathbf{g}^{n+1} = \mathbf{A}^{n+1} + \mathbf{F}^{n+1} + \mathbf{Q}^{n+1} = \mathbf{0}$$

Linearized representation for new state $\mathbf{x}^{n+1}$:

$$\mathbf{g}^{n+1} = \mathbf{0} \approx \mathbf{g}^{i+1} + \frac{\partial \mathbf{g}^{i+1}}{\partial \mathbf{x}^{i+1}}\left(\mathbf{x}^{n+1} - \mathbf{x}^{i+1}\right) + \frac{\partial \mathbf{g}^{i+1}}{\partial \mathbf{x}^{i}}\left(\mathbf{x}^{n} - \mathbf{x}^{i}\right) + \frac{\partial \mathbf{g}^{i+1}}{\partial \mathbf{u}^{i+1}}\left(\mathbf{u}^{n+1} - \mathbf{u}^{i+1}\right)$$

$\mathbf{x}$: states (p, S) $\mathbf{u}$: controls (BHPs)

training run: $(i, i+1)$ test run: $(n, n+1)$

Expansion around Saved States + POD

- Linearized representation (note $\boldsymbol{J}^{i+1} = \partial \mathbf{g}^{i+1} / \partial \mathbf{x}^{i+1}$):

$$\boldsymbol{J}^{i+1}\left(\mathbf{x}^{n+1} - \mathbf{x}^{i+1}\right) = -\left[\frac{\partial \mathbf{g}^{i+1}}{\partial \mathbf{x}^{i}}\left(\mathbf{x}^{n} - \mathbf{x}^{i}\right) + \frac{\partial \mathbf{g}^{i+1}}{\partial \mathbf{u}^{i+1}}\left(\mathbf{u}^{n+1} - \mathbf{u}^{i+1}\right)\right]$$

- Introduce POD basis ($\mathbf{x} = \mathbf{\Phi}\boldsymbol{\xi}$, with $\mathbf{\Phi} \in \mathcal{R}^{2n_b \times l}$ from SVDs of training-run snapshots):

$$\boldsymbol{J}^{i+1}\mathbf{\Phi}\left(\xi^{n+1} - \xi^{i+1}\right) = -\left[\frac{\partial \mathbf{g}^{i+1}}{\partial \mathbf{x}^{i}}\mathbf{\Phi}\left(\xi^{n} - \xi^{i}\right) + \frac{\partial \mathbf{g}^{i+1}}{\partial \mathbf{u}^{i+1}}\left(\mathbf{u}^{n+1} - \mathbf{u}^{i+1}\right)\right]$$

- Now have over-determined system of $\boldsymbol{2n_b}$ equations in $\boldsymbol{l}$ unknowns ($l \ll 2n_b$)

Constraint Reduction for Low-Order System

- Petrov-Galerkin approach: $\boldsymbol{\Psi}^{i+1} = \boldsymbol{J}^{i+1}\boldsymbol{\Phi} \in \mathcal{R}^{2n_b \times l}$

$$\left(\boldsymbol{\Psi}^{i+1}\right)^T \boldsymbol{J}^{i+1}\boldsymbol{\Phi}\left(\boldsymbol{\xi}^{n+1} - \boldsymbol{\xi}^{i+1}\right)$$

$$= -\left(\boldsymbol{\Psi}^{i+1}\right)^T \left[\frac{\partial \mathbf{g}^{i+1}}{\partial \mathbf{x}^i}\boldsymbol{\Phi}\left(\boldsymbol{\xi}^n - \boldsymbol{\xi}^i\right) + \frac{\partial \mathbf{g}^{i+1}}{\partial \mathbf{u}^{i+1}}\left(\mathbf{u}^{n+1} - \mathbf{u}^{i+1}\right)\right]$$

- Solving for $\boldsymbol{\xi}^{n+1}$ (linear, l-dimensional system):

$$\boldsymbol{\xi}^{n+1} = \boldsymbol{\xi}^{i+1} - \left(\boldsymbol{J}_r{}^{i+1}\right)^{-1}\left[\left(\frac{\partial \mathbf{g}^{i+1}}{\partial \mathbf{x}^i}\right)_r \left(\boldsymbol{\xi}^n - \boldsymbol{\xi}^i\right) + \left(\frac{\partial \mathbf{g}^{i+1}}{\partial \mathbf{u}^{i+1}}\right)_r \left(\mathbf{u}^{n+1} - \mathbf{u}^{i+1}\right)\right]$$

$$\boldsymbol{J}_r{}^{i+1} = \left(\boldsymbol{\Psi}^{i+1}\right)^T \boldsymbol{J}^{i+1}\boldsymbol{\Phi} \qquad \left(\frac{\partial \mathbf{g}^{i+1}}{\partial \mathbf{x}^i}\right)_r = \left(\boldsymbol{\Psi}^{i+1}\right)^T \frac{\partial \mathbf{g}^{i+1}}{\partial \mathbf{x}^i}\boldsymbol{\Phi} \qquad \left(\frac{\partial \mathbf{g}^{i+1}}{\partial \mathbf{u}^{i+1}}\right)_r = \left(\boldsymbol{\Psi}^{i+1}\right)^T \frac{\partial \mathbf{g}^{i+1}}{\partial \mathbf{u}^{i+1}}$$

POD-TPWL with Multiple Derivatives

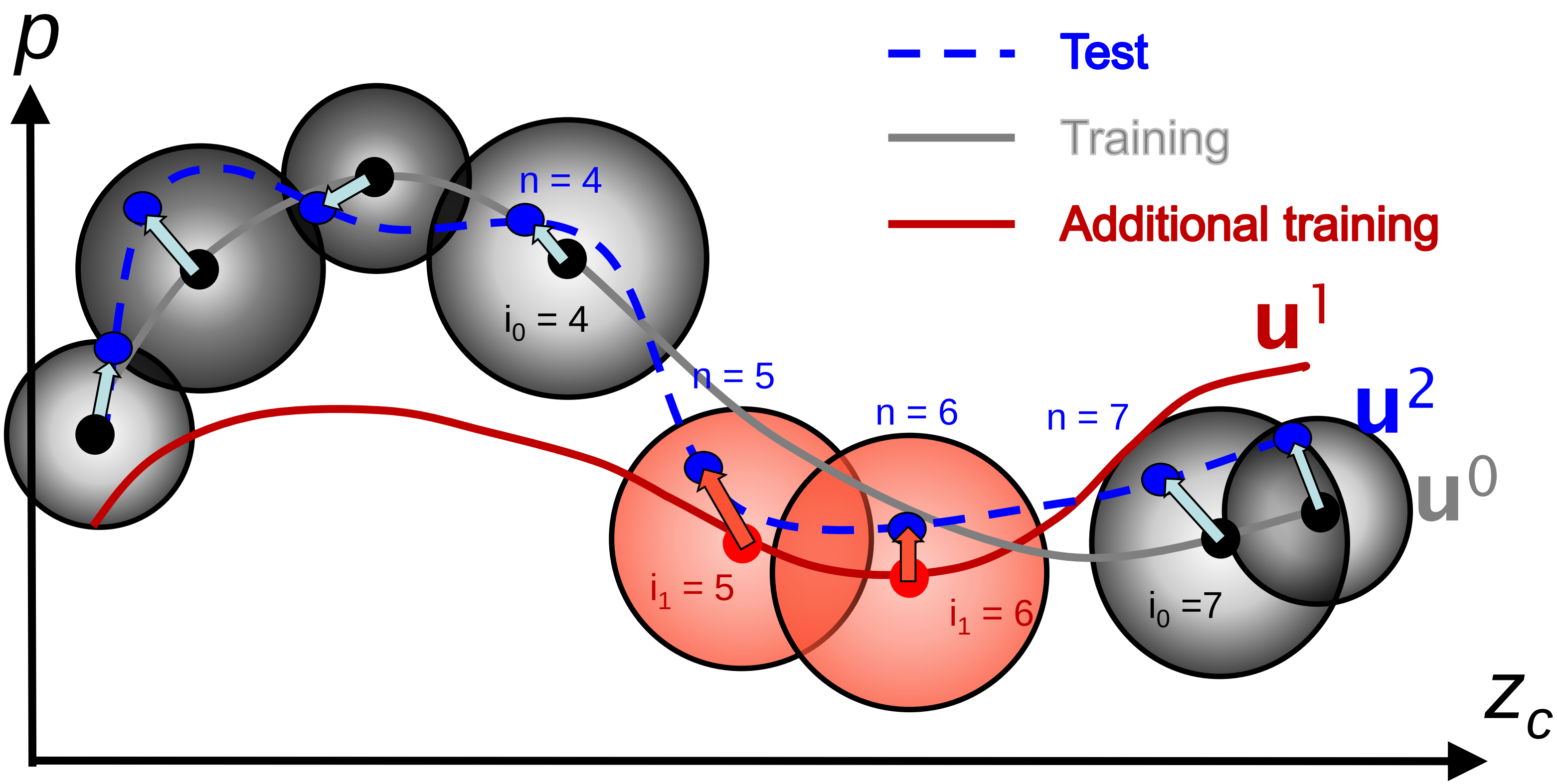

- All trainings provide derivatives and snapshots
- More general ‘point selection’ criteria required

POD-TPWL Flowchart

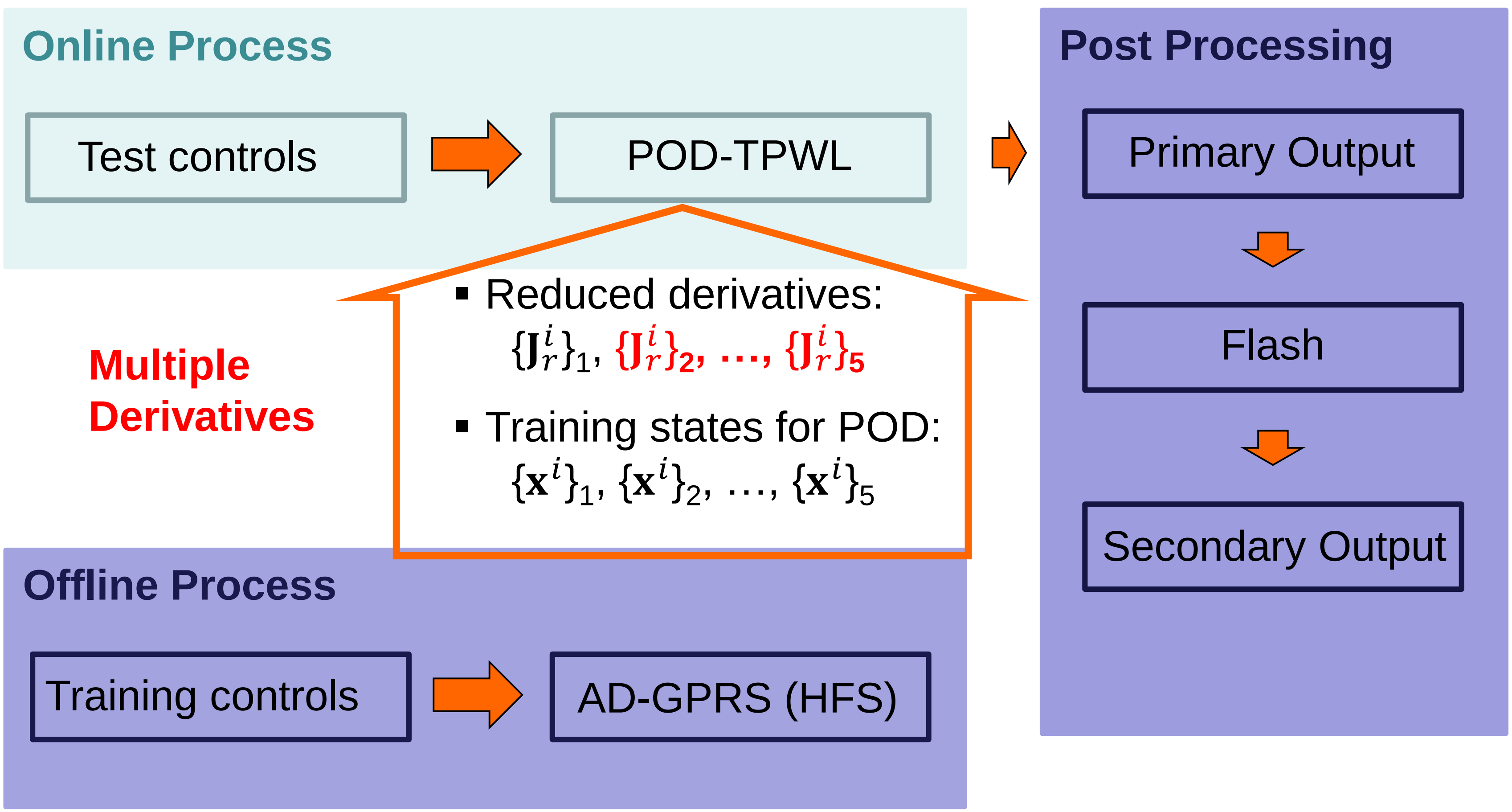

Problem Setup

- Gaussian log-permeability, low-perm at layer 7
- Full model: 43 km x 43 km x 150 m
- Storage aquifer: 2.8 km x 2.8 km x 150 m
- Storage aquifer model: 35 x 35 x 15 blocks

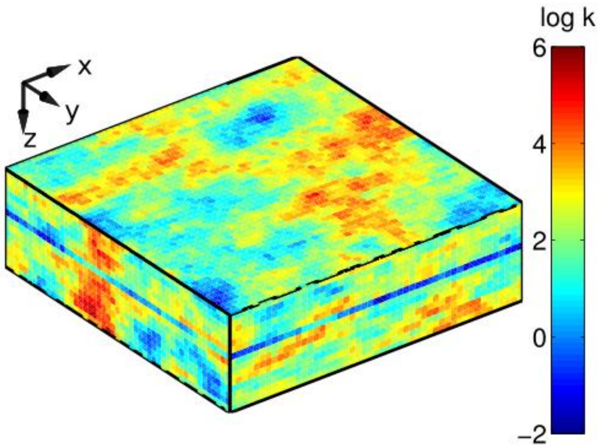

log k_z

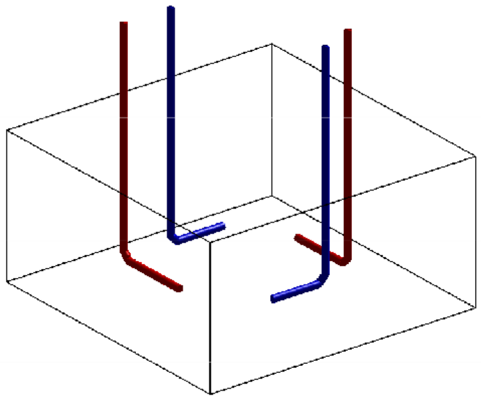

4 horizontal wells

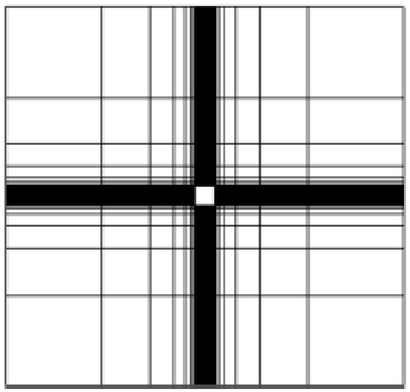

Full model

Training and Test Injection Rates

- Field injection rate: 0.3 million tonnes of CO_2 per year

Training Well 2

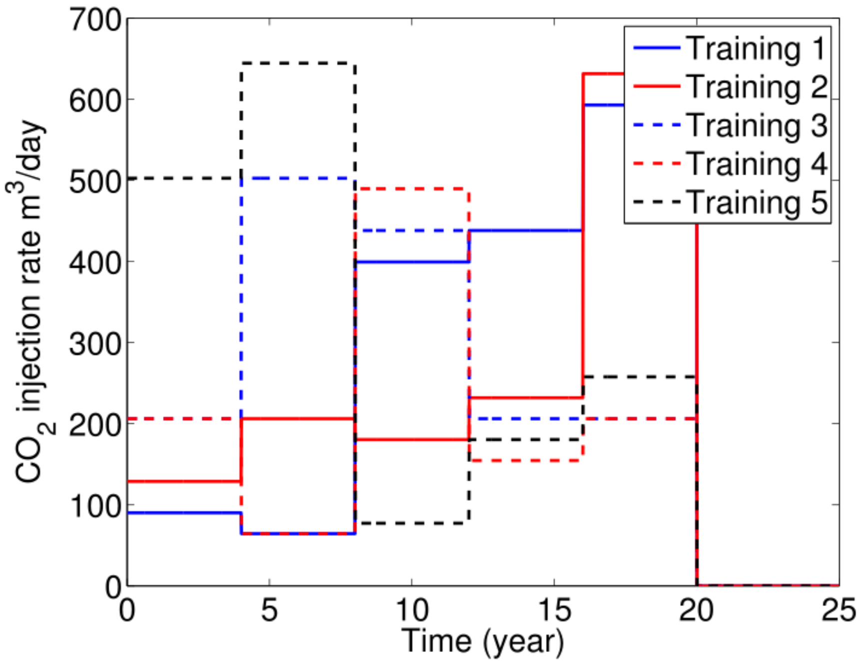

Test Well 2

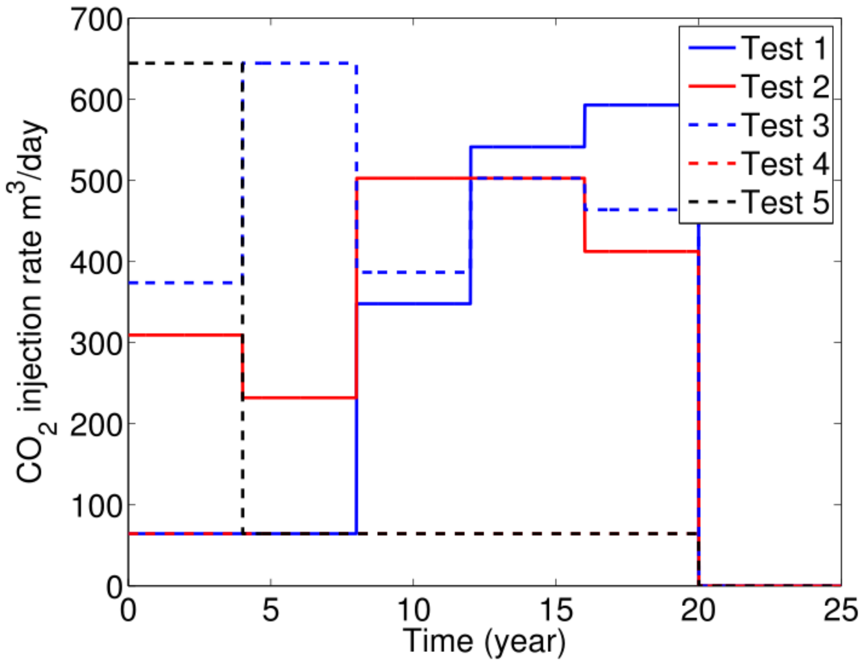

Test Case: BHPs for Well 2

Single derivative

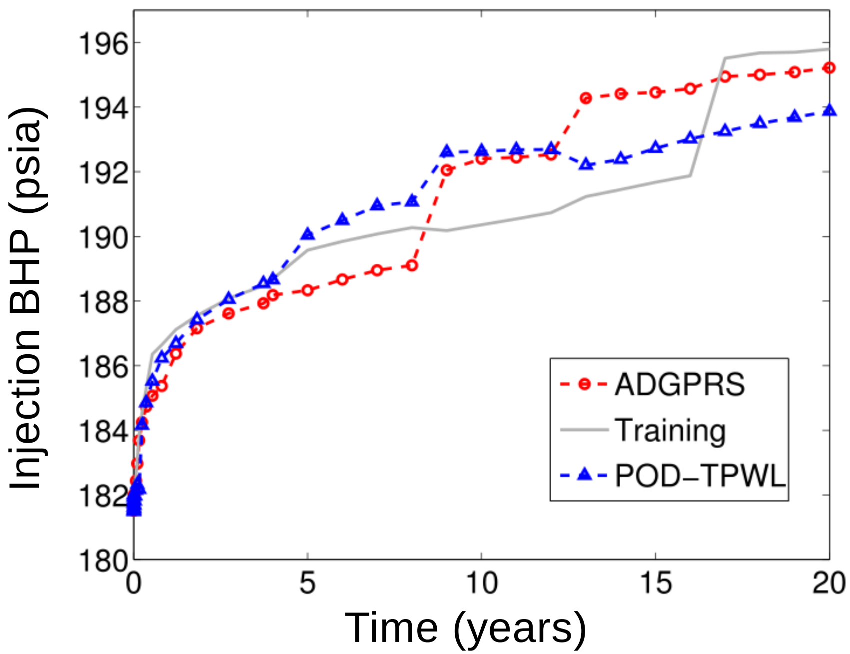

Multiple derivatives

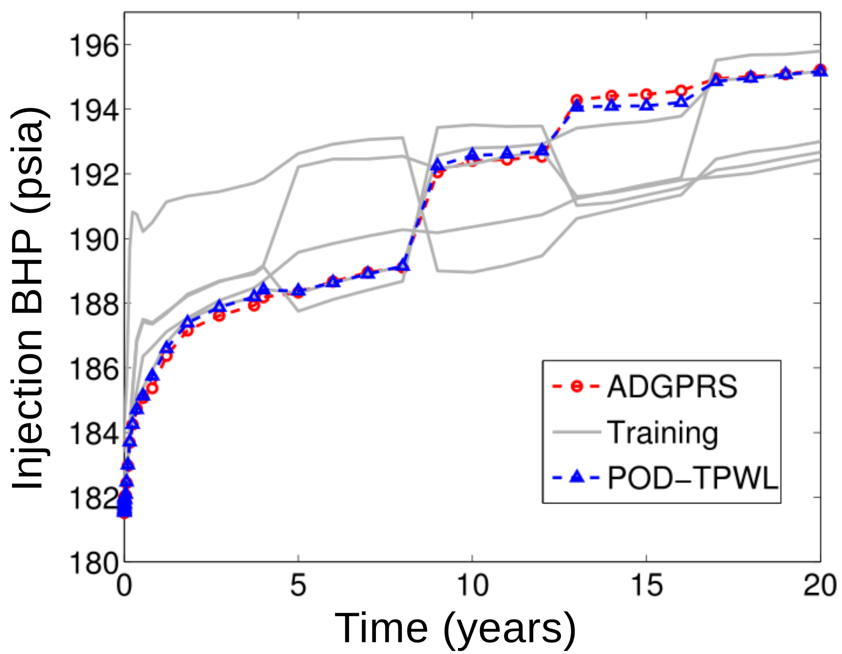

- Single derivative uses snapshots from 5 trainings
- POD-TPWL speed up ~100-150x

CO_2 Molar Fractions at Target Layer (after 20 years)

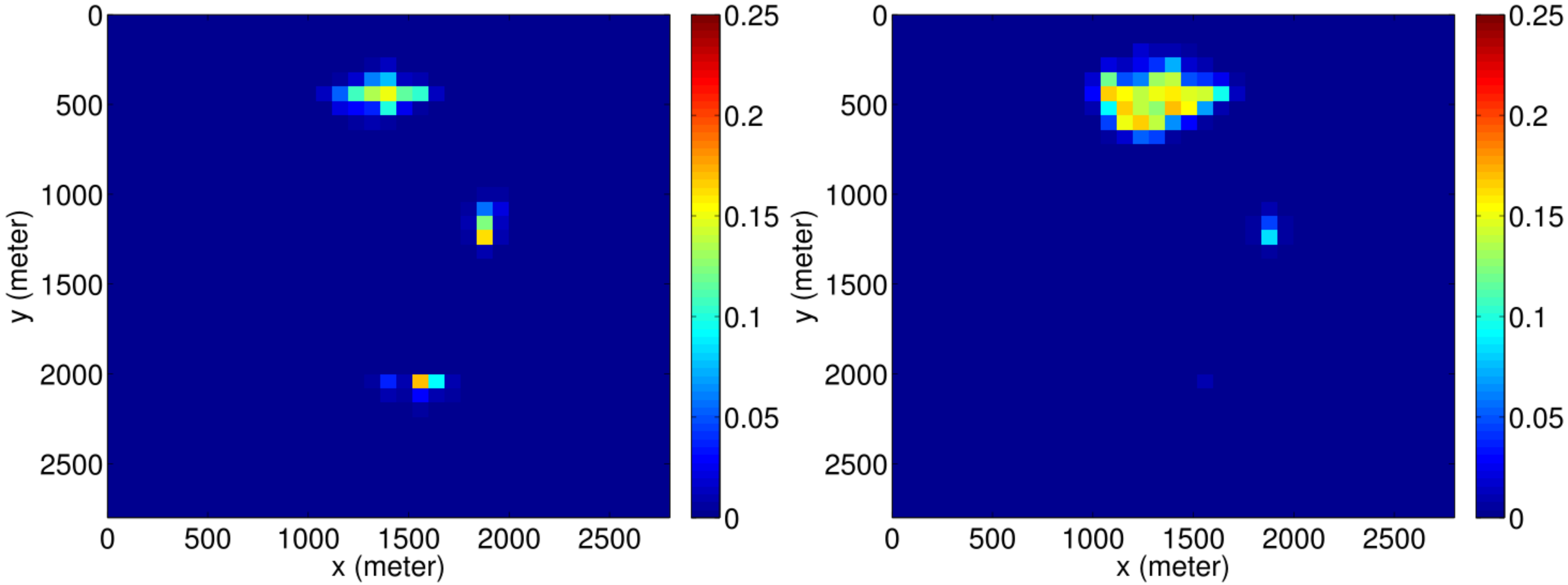

Training (HFS)   Test (HFS)

POD-TPWL Accuracy for Test Run

Single derivative

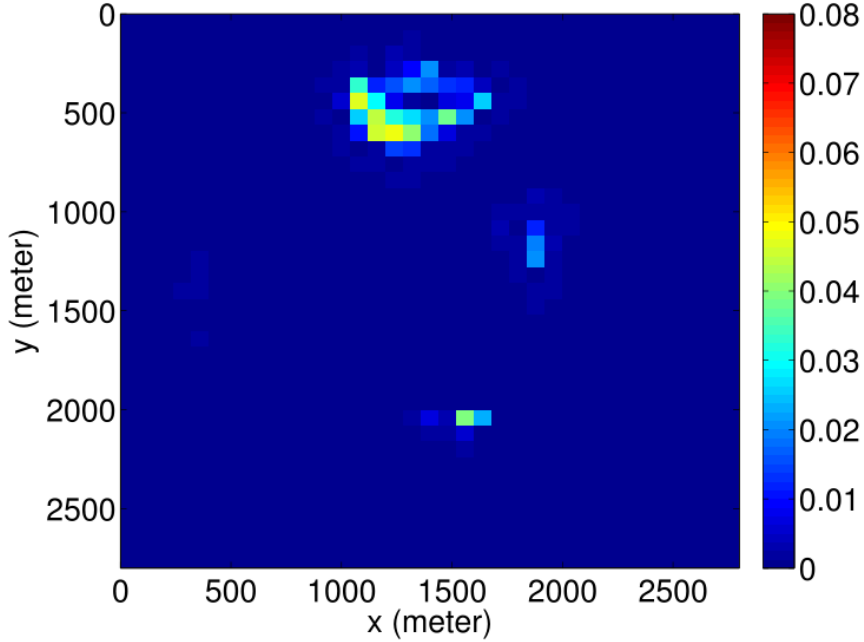

|TPWL – HFS|

Multiple derivatives

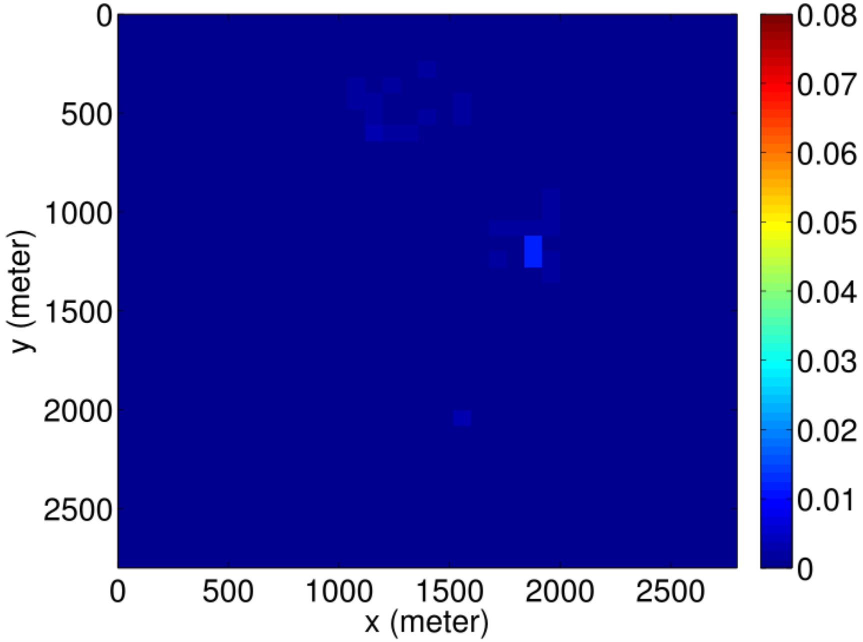

|TPWL – HFS|

Optimization Methodology

- Minimize aggregate CO_2 at target layer
  - Combine MADS (NOMAD) with POD-TPWL
  - Use of multiple derivatives avoids re-training

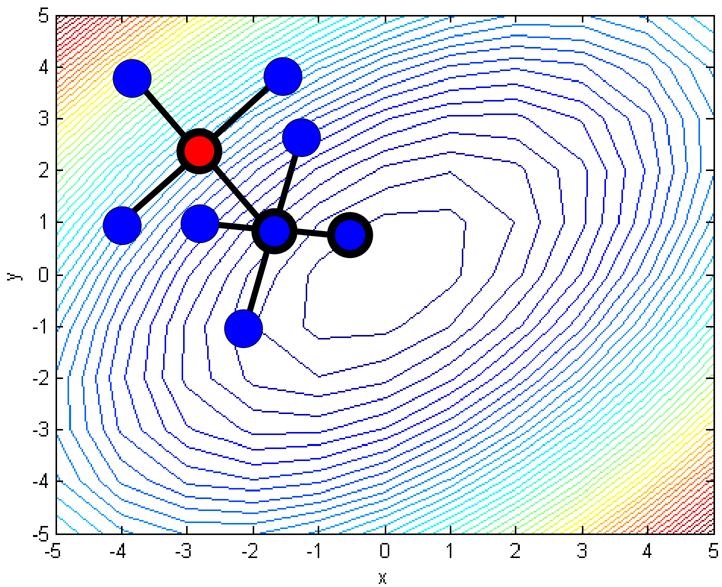

MADS algorithm

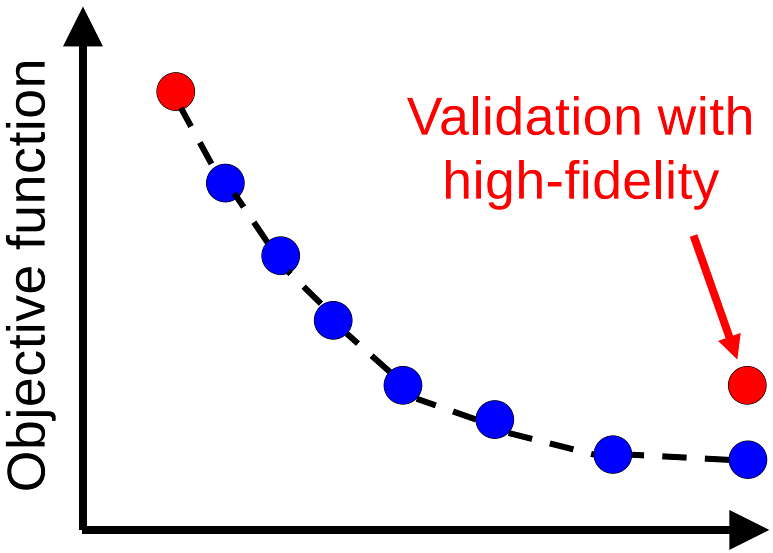

Number of iterations

Optimization Setup

- Channelized aquifer derived from Stanford VI
- Fixed field injection rate, inject for 20 years (2.8% of total PV), 4 control periods, 12 opt. variables)
- 5 training runs (multiple derivatives) for POD-TPWL

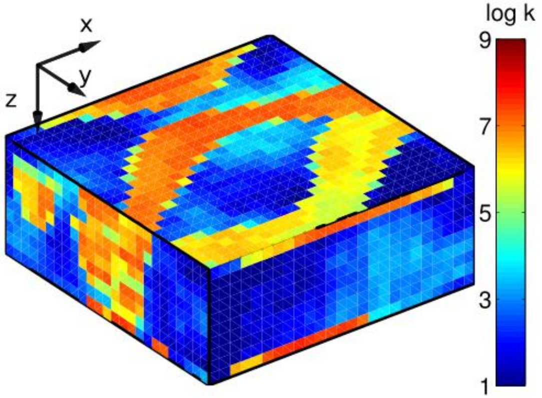

log k_x

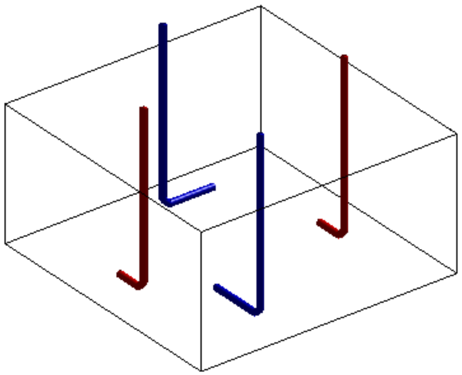

4 horizontal wells

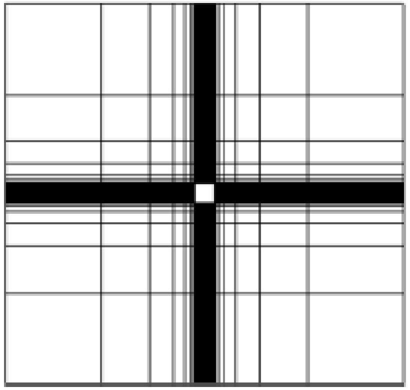

full model

Optimization Results

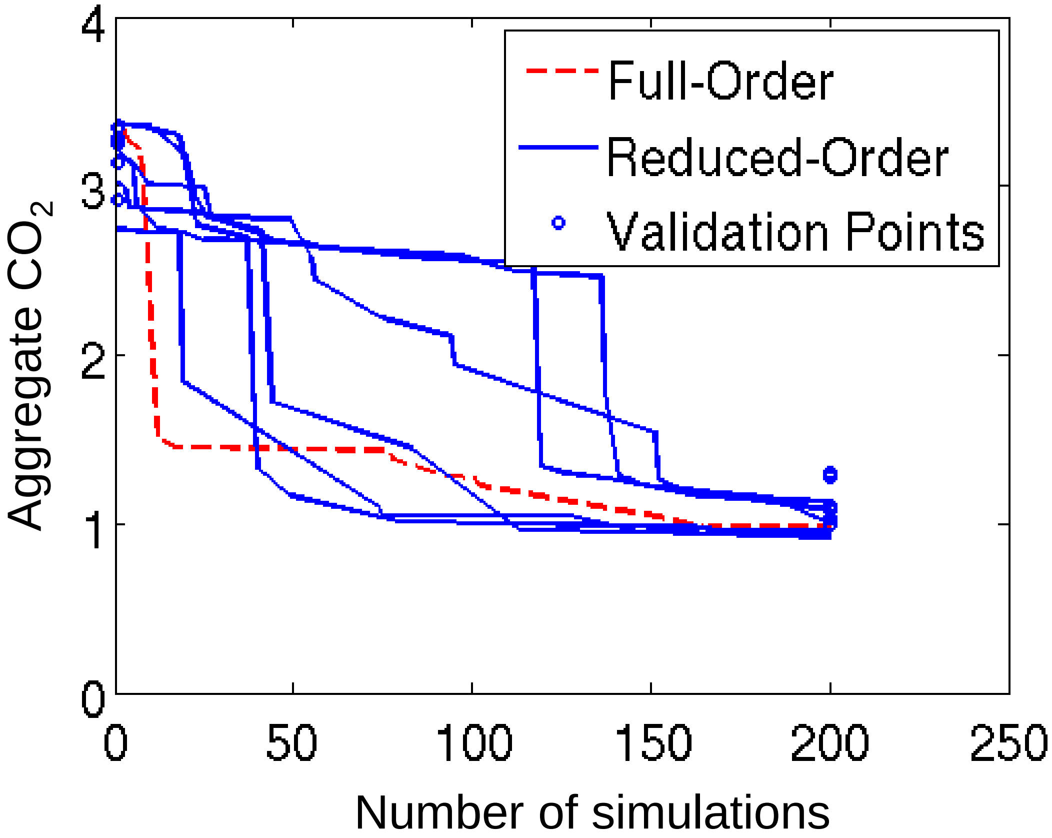

- Full-order: 0.98
- Best POD-TPWL: 0.96

CO_2 Plume Locations (Cross Sections)

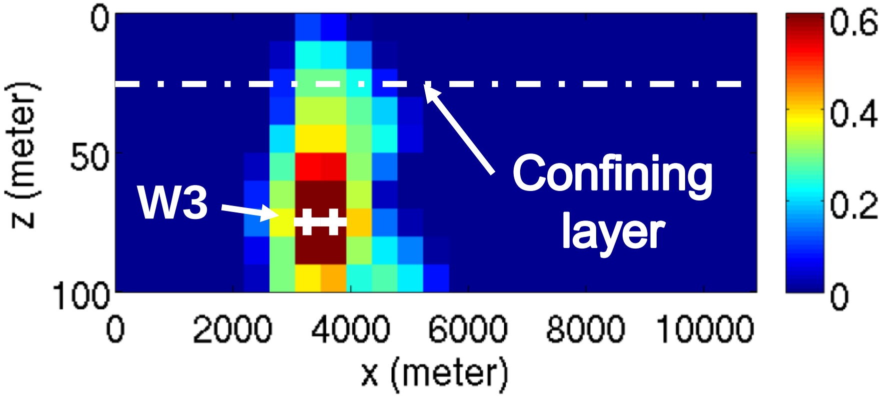

Initial guess, Well 3

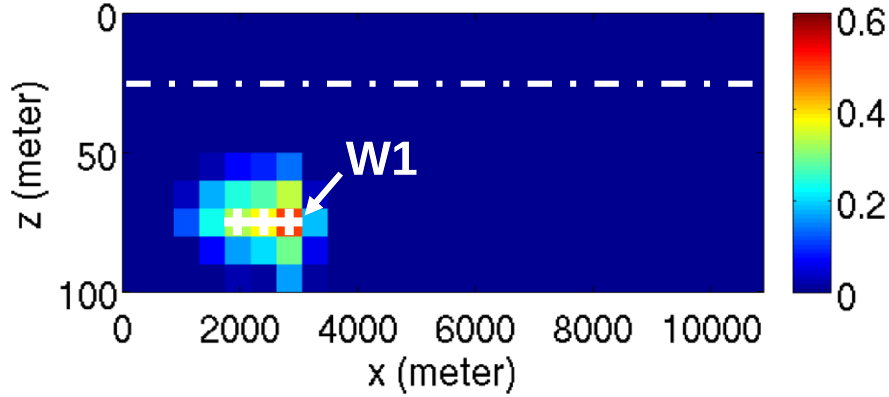

Initial guess, Well 1

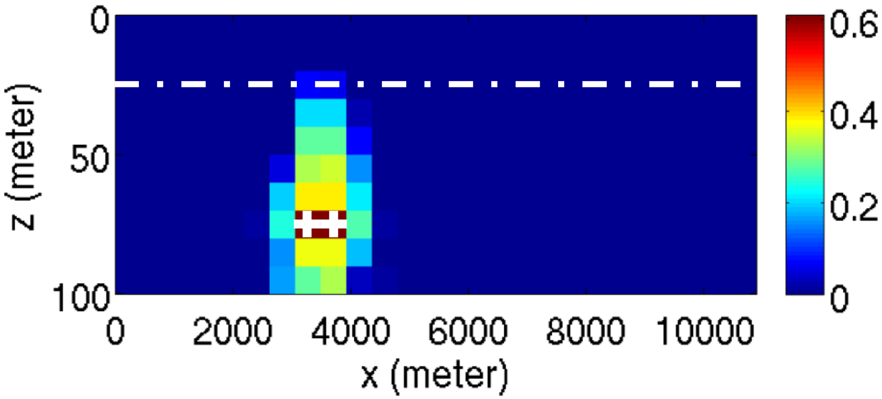

Optimized solution, Well 3

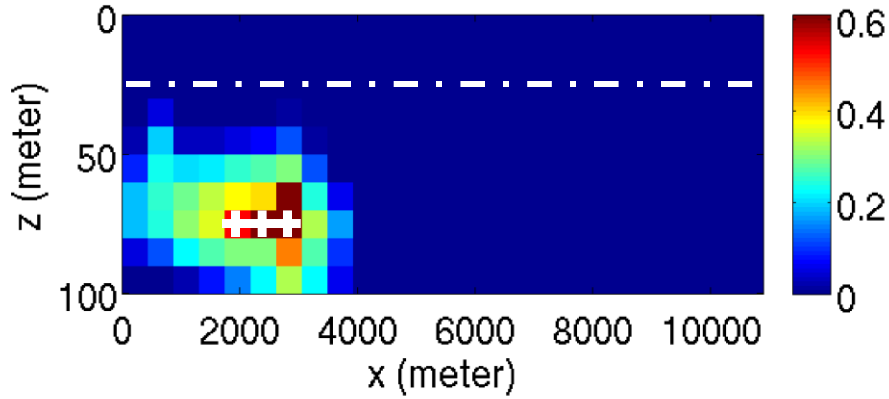

Optimized solution, Well 1

Accuracy of POD-TPWL Solution

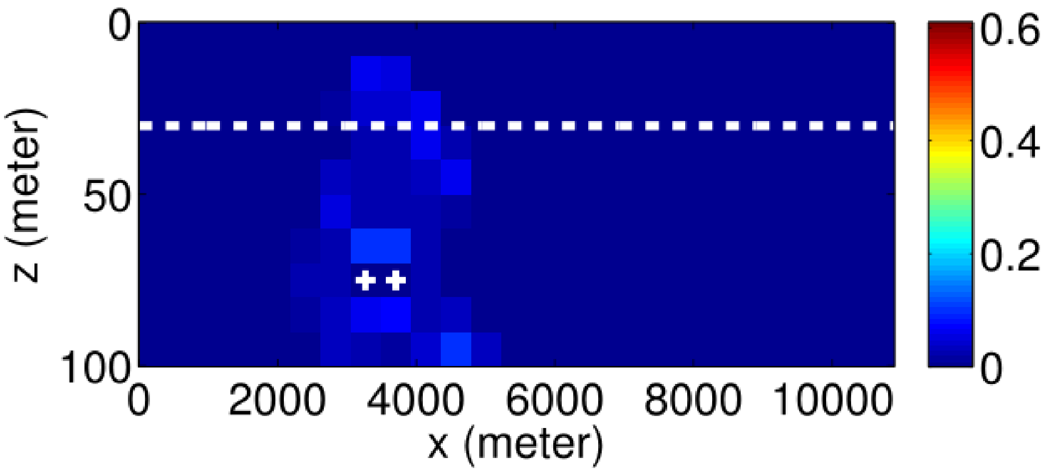

|TPWL – HFS|, Well 3

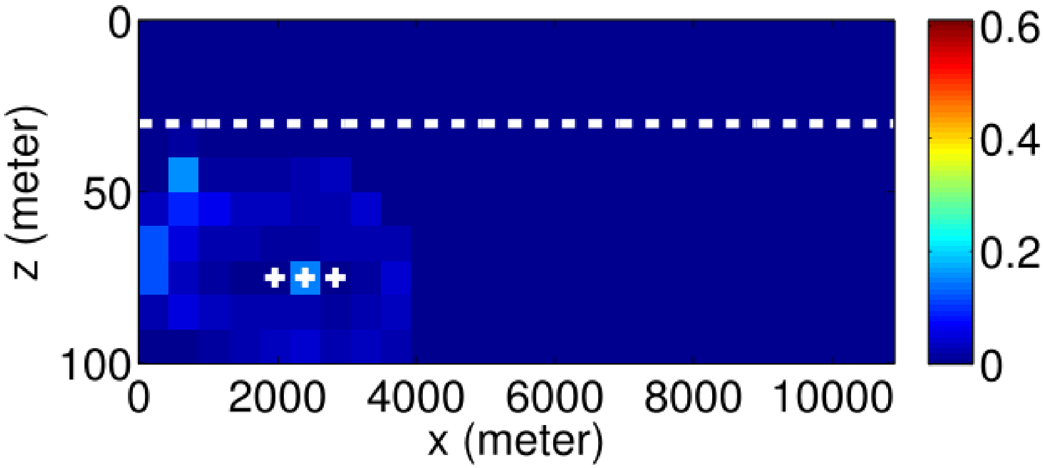

|TPWL – HFS|, Well 1

Second-Order Treatment for Oil-Water Systems

- Quadratic representation for new state $\mathbf{x}^{n+1}$ now includes Hessian-type terms

$$\mathbf{g}^{n+1} = \mathbf{0} \approx \mathbf{g}^{i+1} + \frac{\partial \mathbf{g}^{i+1}}{\partial \mathbf{x}^{i+1}}\left(\mathbf{x}^{n+1} - \mathbf{x}^{i+1}\right) + \frac{\partial \mathbf{g}^{i+1}}{\partial \mathbf{x}^{i}}\left(\mathbf{x}^{n} - \mathbf{x}^{i}\right) +$$

$$\frac{\partial \mathbf{g}^{i+1}}{\partial \mathbf{u}^{i+1}}\left(\mathbf{u}^{n+1} - \mathbf{u}^{i+1}\right) + \frac{1}{2}\frac{\partial}{\partial \mathbf{x}^{i+1}}\left(\frac{\partial \mathbf{g}^{i+1}}{\partial \mathbf{x}^{i+1}}\right)\left(\mathbf{x}^{n+1} - \mathbf{x}^{i+1}\right)\left(\mathbf{x}^{n+1} - \mathbf{x}^{i+1}\right) + \ldots$$

- Introduce POD basis: $\mathbf{x} = \mathbf{\Phi}\boldsymbol{\xi}$
- Apply constraint reduction: pre-multiply by $\left(\mathbf{\Psi}^{i+1}\right)^T$
- Resulting ROM is low-dimensional but nonlinear; solve using Newton’s method

Simulation Results using POD-TPWQ

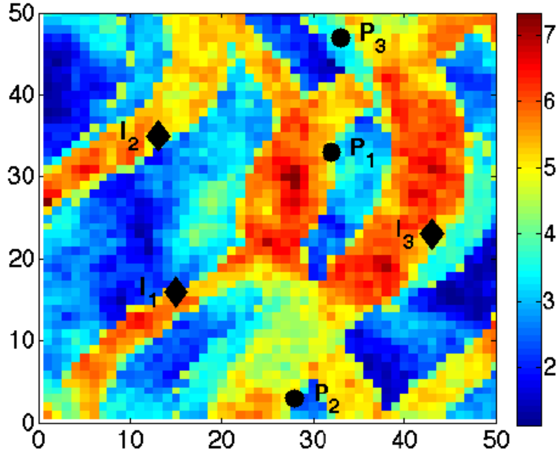

- 2D oil-water simulation
- 3 injectors, 3 producers
- Consider **large BHP perturbation** relative to training run

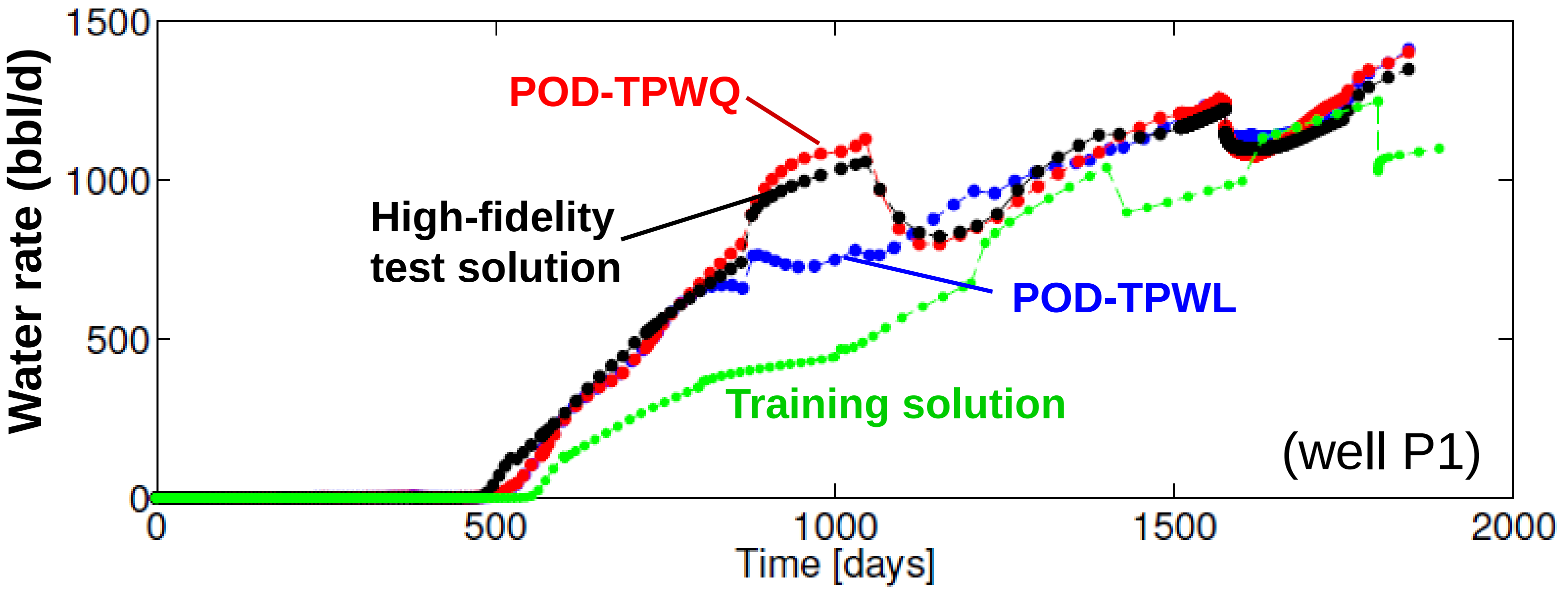

P1 Oil & Water Rates – Larger BHP Perturbations

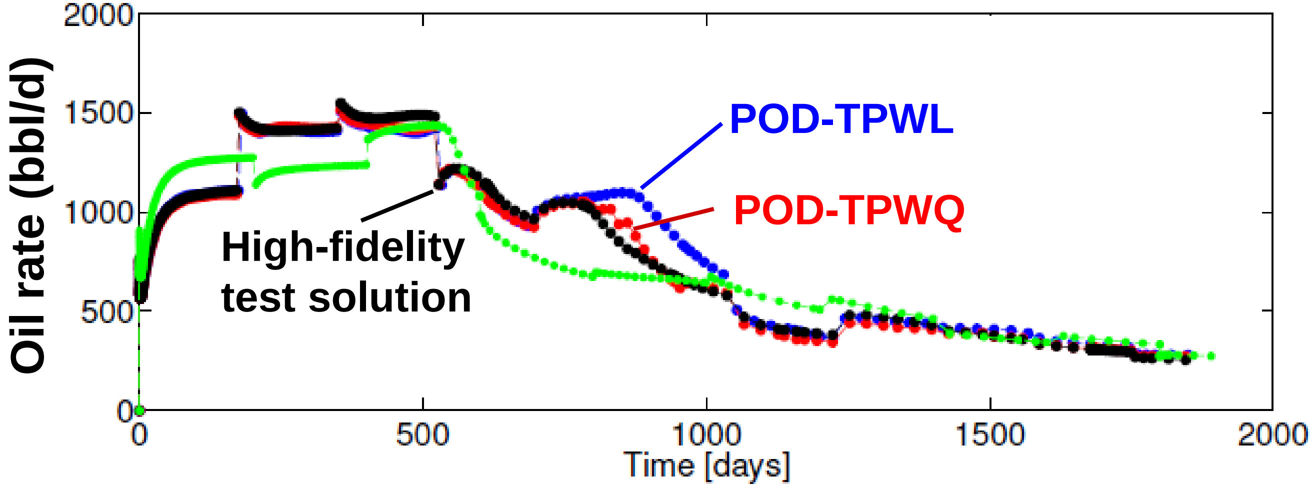

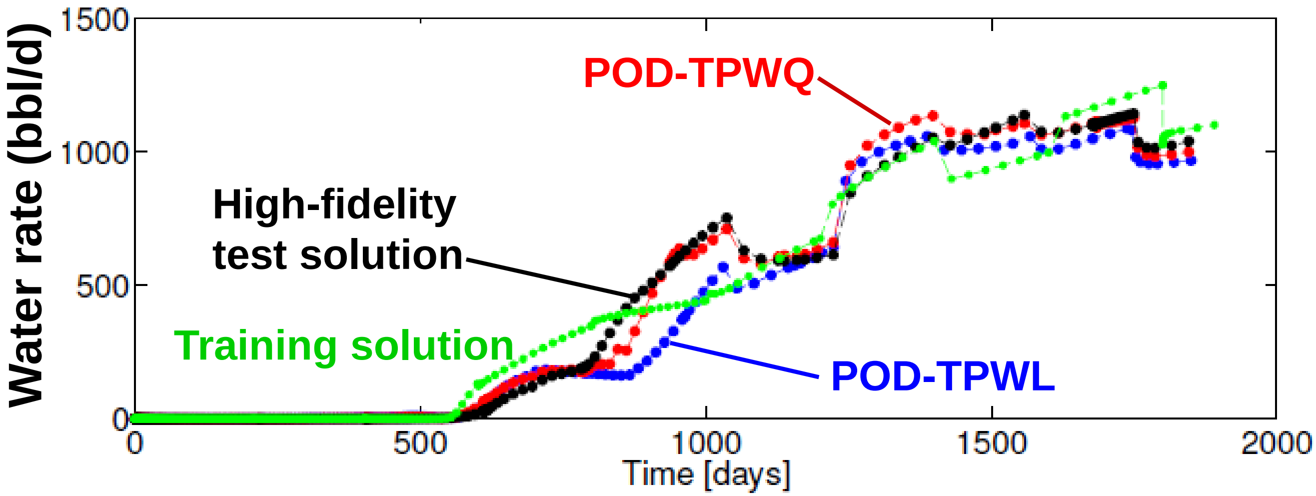

Multifidelity ROM-based Optimization

Perform preprocessing **HFS** (training) runs → Construct **POD-TPWL** & **POD-TPWQ** models

↓

Optimize using **POD-TPWL** model ⇠⇢ Use **POD-TPWQ** as error estimator; retrain with **HFS** as required

↓

Validate optimized solution via **HFS**

- HFS: expensive
- POD-TPWL, POD-TPWQ – inexpensive ROMs
- POD-TPWQ as error estimator

Optimization Problem Setup

- 2D oil-water simulation, maximize NPV
- 2 injectors, 3 producers
- 8 control steps per well → 40 optimization variables
- Numerical gradients from ROM
- Economic parameters – oil: $80/bbl, water cost: $6/bbl

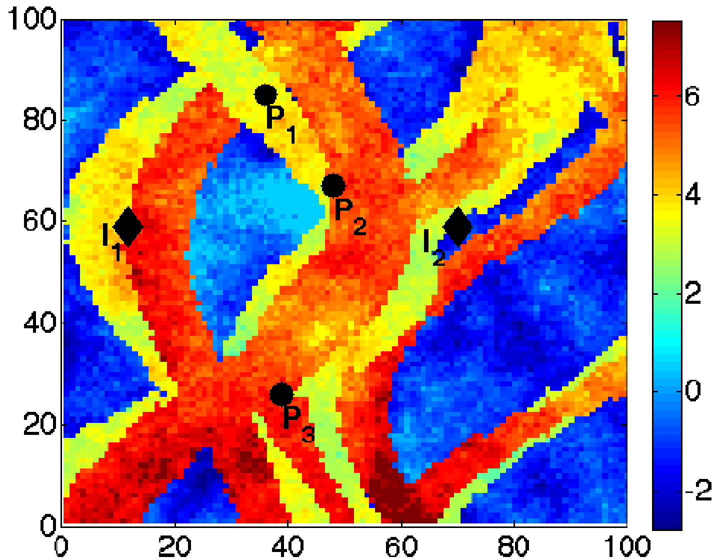

Optimization Results

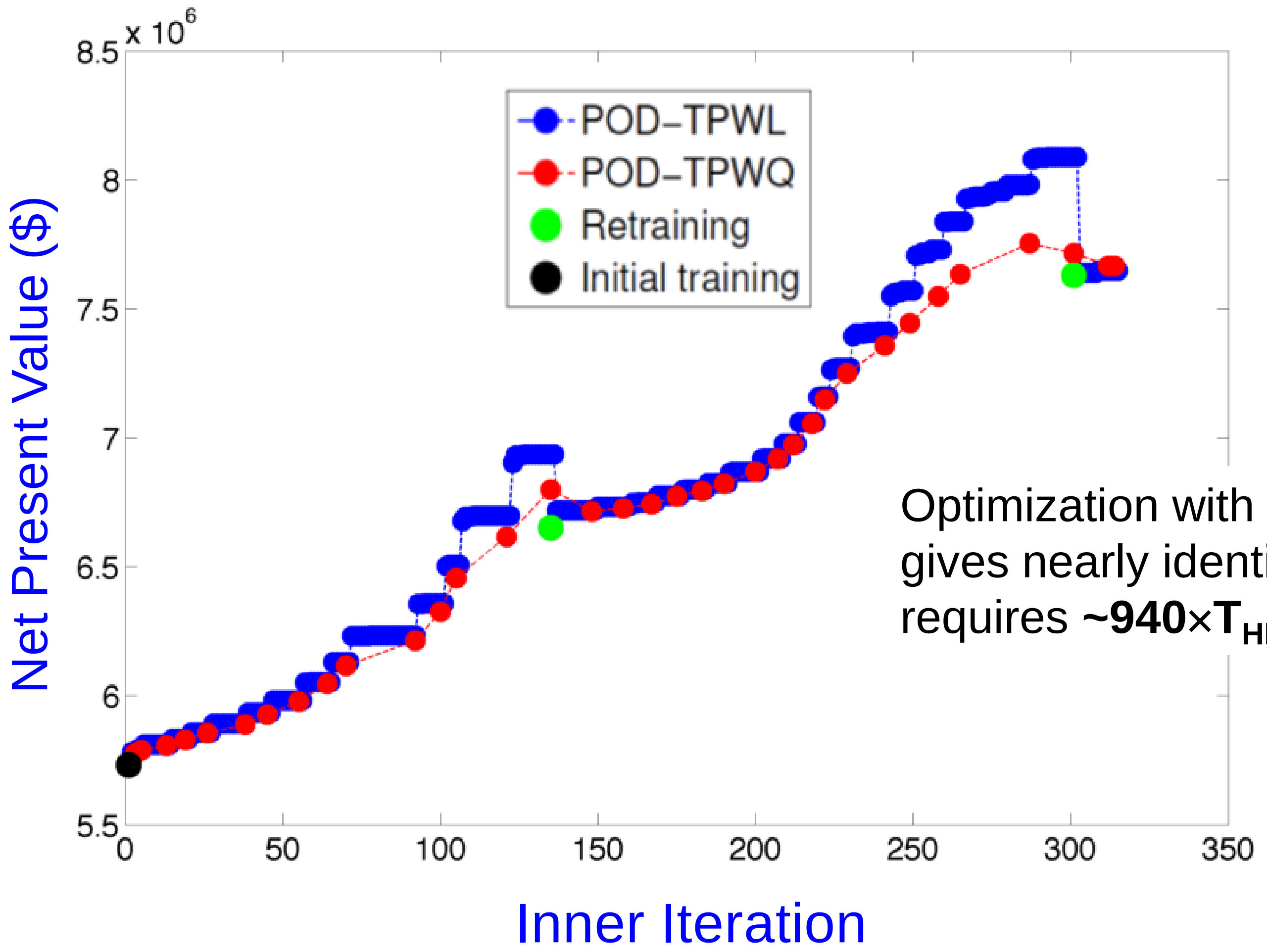

Optimization with HFS gives nearly identical NPV, requires **~940×T_{HFS}**

- ~13,000 POD-TPWL runs, 37 POD-TPWQ runs
- Elapsed time, 12 processors: ~20×T_{HFS} (~50× speedup)

Summary

- Applied computational optimization to minimize risk in carbon storage problems
  - Well locations and time-varying injection rates
  - Brine cycling to further reduce risk
  - Optimization under uncertainty
  - *Leak detection with PCA representation of geology*

- Developed ROM for CO_2 problems (injection stage)
  - Showed benefit of multiple-derivative treatment
  - Employed POD-TPWL in MADS-based optimization

Acknowledgments

- Stanford Smart Fields Consortium
- DOE National Energy Technology Laboratory and Battelle Memorial Institute
- Srikanta Mishra (Battelle)
- Jincong He (now at Chevron)
- Stanford Center for Computational Earth & Environmental Sciences (CEES)

Main References

- Cameron, D.A., Durlofsky, L.J. Optimization and data assimilation for geological carbon storage. *Computational Models for CO_2 Sequestration and Compressed Air Energy Storage*, pp. 357-388, R. Al-Khoury and J. Bundschuh, eds., Taylor & Francis Group/CRC Press (2014).

- Cameron, D.A., Durlofsky, L.J. Optimization of well placement, CO_2 injection rates, and brine cycling for geological carbon sequestration. *International Journal of Greenhouse Gas Control*, **10**, 100-112 (2012).

- Cameron, D.A., Durlofsky, L.J., Benson, S.M. Use of above-zone pressure data to locate and quantify leaks during carbon storage operations. *International Journal of Greenhouse Gas Control*, **52**, 32-43 (2016).

- Zin, Z.L., Durlofsky, L.J. Reduced-order modeling of CO_2 storage operations, in review.

- Trehan, S., Durlofsky, L.J., Trajectory piecewise quadratic reduced-order model for subsurface flow, with application to PDE-constrained optimization. *Journal of Computational Physics*, **326**, 446-473 (2016).

- He, J., Durlofsky, L.J. Reduced-order modeling for compositional simulation by use of trajectory piecewise linearization. *SPE Journal*, **19**, 858-872 (2014).